

See discussions, stats, and author profiles for this publication at: <https://www.researchgate.net/publication/315628469>

# The Gulf Stream frontal system: A key oceanographic feature in the habitat selection of the leatherback turtle?

Article in *Deep Sea Research Part I Oceanographic Research Papers* · March 2017

CITATION

1

READS

376

12 authors, including:



**Philippine Chambault**

University of the Azores, Horta, Portugal

21 PUBLICATIONS 39 CITATIONS

[SEE PROFILE](#)



**Fabien Roquet**

University of Gothenburg

79 PUBLICATIONS 1,488 CITATIONS

[SEE PROFILE](#)



**Alberto Baudena**

Pierre and Marie Curie University - Paris 6

8 PUBLICATIONS 7 CITATIONS

[SEE PROFILE](#)



**Etienne Pauthenet**

Stockholm University

9 PUBLICATIONS 2 CITATIONS

[SEE PROFILE](#)

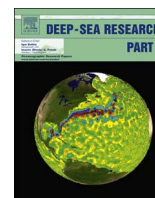
Some of the authors of this publication are also working on these related projects:



Projet INVOCO (Influence des Variables Océanographiques sur le Comportement et la dispersion de la Tortue Caouanne en Méditerranée occidentale [View project](#))



From the Pleistocene to the edge of the sixth extinction crisis: the turbulent history of Northern Amazonian vertebrates [View project](#)



## The Gulf Stream frontal system: A key oceanographic feature in the habitat selection of the leatherback turtle?



Philippine Chambault<sup>a,\*</sup>, Fabien Roquet<sup>b</sup>, Simon Benhamou<sup>c</sup>, Alberto Baudena<sup>d</sup>, Etienne Pauthenet<sup>b</sup>, Benoît de Thoisy<sup>e</sup>, Marc Bonola<sup>a</sup>, Virginie Dos Reis<sup>e</sup>, Rodrigue Crasson<sup>e</sup>, Mathieu Brucker<sup>a</sup>, Yvon Le Maho<sup>a</sup>, Damien Chevallier<sup>a</sup>

<sup>a</sup> Université de Strasbourg, IPHC UMR 7178 F-67000 Strasbourg, France

<sup>b</sup> Stockholm University, Department of Meteorology (MISU), Sweden

<sup>c</sup> Centre d'Étude Fonctionnelle et Évolutive, CNRS, 1919 route de Mende, 34293 Montpellier Cedex, France

<sup>d</sup> Sorbonne Universités, UPMC Université Paris 06, CNRS-IRD-MNHN-IPSL Laboratory, 4 Place Jussieu, F-75005 Paris, France

<sup>e</sup> Association Kwata, 16 avenue Pasteur, BP 672, F-97335 Cayenne Cedex, France

### ARTICLE INFO

#### Keywords:

Post-nesting migration  
*Dermochelys coriacea*  
 North Atlantic  
 Diving behaviour  
 Satellite tracking

### ABSTRACT

Although some associations between the leatherback turtle *Dermochelys coriacea* and the Gulf Stream current have been previously suggested, no study has to date demonstrated strong affinities between leatherback movements and this particular frontal system using thorough oceanographic data in both the horizontal and vertical dimensions. The importance of the Gulf Stream frontal system in the selection of high residence time (HRT) areas by the North Atlantic leatherback turtle is assessed here for the first time using state-of-the-art ocean reanalysis products. Ten adult females from the Eastern French Guianese rookery were satellite tracked during post-nesting migration to relate (1) their horizontal movements to physical gradients (Sea Surface Temperature (SST), Sea Surface Height (SSH) and filaments) and biological variables (micronekton and chlorophyll *a*), and (2) their diving behaviour to vertical structures within the water column (mixed layer, thermocline, halocline and nutricline). All the turtles migrated northward towards the Gulf Stream north wall. Although their HRT areas were geographically remote (spread between 80–30 °W and 28–45 °N), all the turtles targeted similar habitats in terms of physical structures, i.e. strong gradients of SST, SSH and a deep mixed layer. This close association with the Gulf Stream frontal system highlights the first substantial synchronization ever observed in this species, as the HRTs were observed in close match with the autumn phytoplankton bloom. Turtles remained within the enriched mixed layer at depths of  $38.5 \pm 7.9$  m when diving in HRT areas, likely to have an easier access to their prey and maximize therefore the energy gain. These depths were shallow in comparison to those attained within the thermocline ( $82.4 \pm 5.6$  m) while crossing the nutrient-poor subtropical gyre, probably to reach cooler temperatures and save energy during the transit. In a context of climate change, anticipating the evolution of such frontal structure under the influence of global warming is crucial to ensure the conservation of this vulnerable species.

### 1. Introduction

Oceanic fronts are transition areas between water masses of contrasting properties (Belkin et al., 2002; Scales et al., 2014). These sharp boundaries are generally characterized by physical and biological discontinuities in terms of temperature, salinity and nutrient gradients (Le Fèvre, 1986; Reul et al., 2014; Scales et al., 2014; Greer et al., 2015), and occur across a variety of spatial and temporal scales, from sub-mesoscale (1–10s km) to ocean basin scales (1000s km). Oceanic fronts can be generated by various physical processes, ranging from the

presence of an estuary or a shelfbreak, the occurrence of locally enhanced tidal mixing, wind-induced upwelling or convergence patterns, the presence of sea ice or the western intensification of gyre circulations (Belkin et al., 2009).

The physical processes (upwelling, mixing, stirring) generating oceanic fronts lead to increased primary and secondary productivity (Olson and Backus, 1985; Olson et al., 1994), enhancing in most cases the activity at higher trophic levels via bottom-up processes (Le Fèvre, 1986; Largier, 1993; Acha et al., 2004). Frontal systems are therefore commonly associated with a diverse range of marine vertebrates such

\* Corresponding author.

E-mail address: [philippine.chambault@gmail.com](mailto:philippine.chambault@gmail.com) (P. Chambault).

as seabirds (Haney and McGillivray, 1985; van Franeker et al., 2002; Cotté et al., 2007; De Monte et al., 2012; Scheffer et al., 2012; Thorne and Read, 2013; Whitehead et al., 2016), pinnipeds (Bradshaw et al., 2004; Bailleul et al., 2010; Nordstrom et al., 2013), cetaceans (Moore et al., 2002; Etnoyer et al., 2006; Doniol Valcroze et al., 2007; Druon et al., 2012; Murase et al., 2014) and sea turtles (Eckert et al., 2006b; Fossette et al., 2010a; Witherington, 2002; Polovina et al., 2004; Polovina and Howell, 2005).

The largest frontal system in the North Atlantic Ocean is associated with the Gulf Stream, one of the World hydrodynamic oceanic currents (Schmitz and McCartney, 1993; Lozier et al., 1995; Ducet et al., 2000). Forming the western boundary current system of the North Atlantic Ocean subtropical gyre, this fast current originates in the Gulf of Mexico and intensifies along the south-east coast of the United States before leaving the coastline to cross the Atlantic Ocean at about 40 °N. A strong thermal boundary occurs at the intersection of the warm, salty Gulf Stream waters and the cold and less salty waters of the Labrador Current (Fuglister, 1963). Like in other frontal systems, some associations have been observed between the Gulf Stream and marine megafauna (Olson et al., 1994) such as seabirds (Haney and McGillivray, 1985; Thorne and Read, 2013), fish (Block et al., 2001, 2005; Wilson et al., 2004; Skomal et al., 2009; Potter et al., 2011) and sea turtles (loggerhead: Witherington, 2002; leatherback: Eckert et al., 2006b; Fossette et al., 2010a; Lutcavage, 1996; Dodge et al., 2014).

While the leatherback turtle (*Dermochelys coriacea*) has often been tracked in the Atlantic Ocean (Bailey et al., 2012b; Eckert et al., 2006b; Fossette et al., 2010b, 2010a; James et al., 2005a, 2005b; Ferraroli et al., 2004; Hays et al., 2004; McMahon and Hays, 2006; López-Mendilaharsu et al., 2009; Dodge et al., 2014), only a few studies have suggested that this species may associate with the Gulf Stream frontal system (Eckert et al., 2006b; Fossette et al., 2010a; Lutcavage, 1996). More recently, Dodge et al. (2014) have shown a relationship between leatherback movements and strong Sea Surface Temperature (SST) gradients, highlighting some affinities for the Gulf Stream front, but only for a limited number of individuals ( $n=2$ ), and not in the vertical dimension. Given that the Gulf Stream frontal system is marked by strong SST gradients and pronounced vertical mixing, aggregating therefore low trophic level organisms such as jellyfish (Sims and Quayle, 1998; Greer et al., 2013; Powell and Ohman, 2015), it would be logical to expect North Atlantic leatherback turtles to interact with the Gulf Stream frontal system during their post-nesting migration across the North Atlantic. We propose in this study to examine more systematically the potential affinities of leatherback turtles with this frontal system based on detailed 3D oceanographic data, investigating both the geographical patterns and the vertical dive behaviour in relation to physical and biological ocean conditions.

This study assesses the role of the Gulf Stream frontal system in the selection of preferentially used areas by the leatherback turtle via the satellite tracking of 10 adult females, equipped between 2014 and 2015 from the Eastern French Guianese rookery. This is one of the two major rookeries for the leatherback turtle on the west coast of the equatorial Atlantic (Fossette et al., 2008), showing a different genetic structuration (Molfetti et al., 2013). Note that several female leatherback turtles from the Western French Guianese population have been tracked in the past (Fossette et al., 2010b, 2010a), but it is the first time tracks from the Eastern rookery are documented. After identifying high residence areas (a proxy of foraging grounds), we used a series of biological and physical variables provided by 3D ocean reanalysis products to relate (1) the horizontal movements of the leatherback turtles to physical properties (SST and Sea Surface Height (SSH) gradients and filaments) and biological variables (micronekton and chlorophyll *a*), and (2) their diving behaviour to vertical structures within the water column (mixed layer, thermocline, halocline and nutricline).

## 2. Materials and methods

### 2.1. Ethics statements

This study met the legal requirements of the country in which the work was carried out (France), and followed all institutional guidelines. The protocol was approved by the “Conseil National de la Protection de la Nature” (CNP, <http://www.conservation-nature.fr/acteurs2.php?id=11>), which is under the authority of the French Ministry for ecology, sustainable development and energy (permit Number: 2015133-0022), and acts as the ethics committee for French Guiana. The fieldwork was carried out in strict accordance with the recommendations of the Police Prefecture of Cayenne (French Guiana, France), to minimize any disturbance of the animals.

### 2.2. Study area and tag deployment

During the 2014 and 2015 nesting seasons, 11 adult female leatherback turtles were equipped with satellite tags on the beaches of Rémire-Montjoly (4.53°N–52.16°W, Cayenne, French Guiana). One Argos Fastloc GPS tag (SPLASH10-F-296A, Wildlife Computers Redmond, WA, USA) was deployed in August 2014 and 10 Satellite Relay Data Loggers (SRDL, Sea Mammal Research Unit, University of St. Andrews, Scotland) were deployed in June 2015. These tags were attached during night-time egg laying, i.e. at the only moment when individuals are static while ashore. Harnesses were not used to attach the satellite tags in order to minimize hydrodynamic drag. Prior to attachment, the tags were moulded into a resin mount to match the shape of the central dorsal ridge, and two holes were drilled into the resin mount for the stainless steel cable. The attachment area was disinfected with Betadine then locally anesthetised with Lidocaïne © spray. Two < 0.5 cm diameter holes were drilled into the central dorsal ridge. The tags were then fixed by threading a stainless steel cable through the holes in the dorsal ridge and the resin tag mount. Stainless steel crimps were used to secure the cable and were covered with an epoxy resin to ensure solidity, preventing the tag from being released before the return of the turtles to the nesting site (French Guiana) in 2–4 years.

### 2.3. Data collected from the tags

Both tag types recorded horizontal (Argos and/or GPS locations) and vertical movements (diving behaviour) of the turtles, but at different resolutions.

#### 2.3.1. Argos Fastloc GPS tag

The single Argos Fastloc GPS tag deployed in 2014 recorded both Argos and GPS locations (every 4-h), as well as depth data describing specific diving parameters, namely maximum dive depths, dive durations, and *in situ* temperature data, binned as 4-h period histograms. The wet/dry sensor of the tag was used to identify the beginning and end of each dive. The sensor entered haul-out state after 20 consecutive dry minutes, and exited haul-out state if it remained wet for 30 s or more. Maximum depths were collected in different bins, every 10 m from 10 to 100 m, then every 50 m from 100 to 250 m with a depth sensor accuracy of 1% of reading. Similarly, maximum dive durations were stored from 30 s to 1 min, then every minute from 1 to 5 min, every five minutes from 5 to 20 min, and *in situ* temperatures from 20 to 32 °C were recorded during dives with a resolution of 1 °C, with a temperature sensor accuracy of 0.1 °C. This tag also supplied Time At Depth (TAD), defined as the proportion of time (in %) spent at each depth.

#### 2.3.2. SRDL tags

One of the 10 SRDL tags deployed in 2015 did not transmit any data, and was therefore excluded from the analysis. The other nine SRDL tags provided Argos-based location data, as well as data about

diving behaviour including dive depth (with a depth sensor resolution of 0.5 m), dive duration and duration of post-dive surface intervals. The wet/dry sensor of the tag was used to identify the beginning and end of each dive. Dives started when the sensor was wet and below 1.5 m for 20 s, and ended when dry or above 1.5 m. The SRDL tags were programmed to send summarized dive profiles using the compression algorithm described by Fedak et al. (2001), with 4 depth records for each dive (instead of 1 maximum depth per dive for the Argos Fastloc GPS tag).

## 2.4. Data pre-filtering

As all tags were deployed during the nesting season, they recorded movements and diving behaviour for both the nesting and migration phases. Following the procedure described in Chambault et al. (2015), we excluded the nesting phase to focus on the migration phase alone. A Kalman filtering algorithm (Silva et al., 2014; Lopez et al., 2014) provided by Collecte Location Satellites (CLS Toulouse, France) was applied to estimate Argos locations. Basically, the algorithm uses a correlated random walk model to predict the next location and its associated error based on the previous positions and estimated error. To each Argos location was assigned a Location Class (LC): 3, 2, 1, 0, A, B or Z. Approximately 17% of the locations of our study were associated with an estimated error (from > 250 m to > 1500 m, LC 3: 2.1%, 2: 4.3%, 1: 5.6% and 0: 5.7%), 83% had no accuracy estimation (LC A: 20.5% and B: 61.7%), and 1% were invalid (LC Z). The GPS locations (provided by the single tag deployed in 2014) were associated with an accuracy < 100 m (0.1% recorded). We used the General Bathymetric Chart of the Oceans (GEBCO) database (<http://www.gebco.net/>, resolution 30 arc-second, ~1 km grid) to discard any locations on land. As described in Fossette et al. (2010a), we also discarded the Argos locations associated with a speed of over 10 km h<sup>-1</sup> (9% in 2014 and 10% in 2015, Fossette et al., 2010b), as well as “type Z” (i.e. invalid Argos-based) locations.

## 2.5. Current correction of tracks

Tracks were first re-sampled according to the mean daily locations frequency obtained for both tag types: every 2 h (Argos-GPS) or 8 h (SRDL). We then corrected the ground-related (satellite-recorded) tracks for oceanic currents to estimate the movements of leatherbacks according to the water masses they cross, providing a more accurate picture of actual movement behaviour (Girard et al., 2006; Gaspar et al., 2006). Surface current velocity fields can be computed as the vectorial sum of geostrophic and Ekman components (Sudre et al., 2013). The geostrophic component results from the balance between the horizontal pressure gradient force and the Coriolis force. It was computed from the Ssalto/Duacs maps of absolute dynamic topography data available daily on a 1/4 ° grid ([www.avisio.altimetry.fr/en/data/products/sea-surface-height-products/global/madt-h-uv.html](http://www.avisio.altimetry.fr/en/data/products/sea-surface-height-products/global/madt-h-uv.html)) based on an updated assessment of the sum of sea level anomalies and mean dynamic topography, both being referenced over a twenty-year period in the Duacs 2014 version (V15.0). The Ekman component results from the balance between friction by wind and the Coriolis force. It was estimated from wind stress data provided daily on a 1/4° grid by CERSAT IFREMER (Ascat daily gridded mean wind field: <http://cersat.ifremer.fr/data/products/catalogue>). Both geostrophic and Ekman components were computed using a recent model (GEKCO product) developed by Joël Sudre and underwent a bi-linear spatial interpolation and a linear temporal interpolation to estimate their “meridional” (i.e. E-W) *U* and “zonal” (i.e. S-N) *V* components at every turtle's location (velocity field data and a user-friendly program to interpolate local values at any location and time are freely available at [www.legos.obs-mip.fr/sudre](http://www.legos.obs-mip.fr/sudre)). It is worth noting however that the Ekman component becomes negligible under the mixed layer (e.g. within the thermocline, Marshall and Plumb, 2007). We therefore estimated the proportion *P* of time spent above the thermocline for

each dive of each turtle, and computed the real current velocity as:

$$U_{actual} = U_{geostrophic} + P \cdot U_{Ekman} \quad \text{and} \quad V_{actual} = V_{geostrophic} + P \cdot V_{Ekman}$$

The time spent above the thermocline could not be calculated for the Argos-GPS tag deployed in 2014 due to the coarser resolution of the diving data. For this turtle, *P* was estimated as a function of the location based on the diving data provided by the 9 other tags. Finally, the water mass-related (i.e. “motor”) step lengths for each turtle were computed as:

$$\Delta X_{motor} = \Delta X_{track} - \Delta t \cdot U_{actual} \quad \text{and} \quad \Delta Y_{motor} = \Delta Y_{track} - \Delta t \cdot V_{actual}$$

where  $\Delta X_{track}$  and  $\Delta Y_{track}$  are ground-related step lengths based on coordinates of the satellite-recorded locations (converted from longitude and latitude to an orthonormal metric system *X* and *Y*), and  $\Delta t$  is the time of movement between a given location and the next (see Girard et al., 2006 for details).

## 2.6. Residence time analysis

We inferred high residence time (HRT) phases (and therefore HRT areas) by applying Residence Time (RT) analysis (Barraquand and Benhamou, 2008; Benhamou and Riotte-Lambert, 2012) to the current-corrected movements. The RT for a given location indicates the time spent within a circle centred on this location with a given radius *R*. It is therefore computed as the difference between forward and backward first passage times at distance *R* from the centre, plus possible additional backward and/or forward times spent within the circle provided that the animal does not leave the circle for more than a given time (set to 8 h in the present study), before returning within the circle. The circle runs along the path in this approach, providing a more contrasted and less noisy time series (with respect to simpler analyses based on first passage times). As advised in Barraquand and Benhamou (2008), we computed RT time series with a radius *r* ranging between 10 and 100 km to explore different scales. The low residence time (hereafter LRT) and HRT areas for the migration of each turtle were then inferred by segmenting RT time series using Lavielle (2005) segmentation method.

## 2.7. Environmental data

### 2.7.1. Horizontal variables

We extracted a series of environmental variables from both remote sensed data and model simulations to characterize the habitat of leatherback turtles at their HRT areas. The variables selected were those most likely to influence the distribution of jellyfish (Graham et al., 2001). We extracted the surface sea water chlorophyll *a* concentration at each turtle location from the *Global ocean biochemical analysis and forecast* product (BIO 001–014) at a 0.5 ° spatial resolution (from U.E Copernicus Marine Service Information: <http://marine.copernicus.eu/services-portfolio/access-to-products/>).

As the *Spatial Ecosystem And Population Dynamics Model* (SEAPODYM) predicts the spatio-temporal distribution of micronekton (Lehodey et al., 2008, CLS Toulouse), the smallest pelagic organisms capable of swimming against sea currents (individuals measuring from 2 to 25 cm), it was used to estimate the distribution of leatherback prey. It includes the diet of leatherback turtles and encompasses different micronekton groups, including jellyfish (Brodeur et al., 2005). Micronekton is modelled using current and temperature data provided by the *Global Ocean Reanalysis and Simulations* product (GLORYS-2v1), and net primary production and euphotic depth derived from ocean colour satellite data (<http://www.science.oregonstate.edu/ocean.productivity/>) using the *Vertically Generalised Production Model* (VGPM). Due to the lack of micronekton predictions in nearshore mesopelagic and bathypelagic layers, we estimated only the epipelagic layer using this model. To investigate variations in the vertical accessibility of leatherback prey, we also extracted the euphotic depth weekly on a grid of 0.25 ° × 0.25 °.

**Table 1**

Summary of the horizontal post-nesting movements of the 10 leatherback turtles tracked. Speed values are Mean  $\pm$  SD. PTT refers to the turtle's ID, Nloc to the number of locations, HRT to high residence time.

PTT	Tag type	Start date	End date	Nloc	Tracking duration (d)	Distance (km)	Daily speed (km d <sup>-1</sup> )	Duration to HRT areas (d)
131347	SPLASH10-F	28/08/2014	25/01/2015	1798	150	6794	44.9 $\pm$ 29.0	92
149680	SRDL	30/07/2015	06/11/2015	297	99	4957	49.6 $\pm$ 25.9	65
149681	SRDL	06/07/2015	12/12/2015	479	159	7122	44.5 $\pm$ 21.4	92
149682	SRDL	18/07/2015	03/02/2016	579	200	8080	40.8 $\pm$ 34.0	111
149683	SRDL	16/07/2015	12/11/2015	357	119	5093	42.4 $\pm$ 19.6	79
149684	SRDL	08/07/2015	07/12/2015	454	152	7093	46.3 $\pm$ 22.8	115
149685	SRDL	14/07/2015	21/02/2016	665	222	11640	52.2 $\pm$ 27.1	73
149687	SRDL	26/06/2015	26/12/2015	547	183	11181	60.8 $\pm$ 24.8	66
149688	SRDL	08/07/2015	14/04/2016	844	281	11066	39.2 $\pm$ 21.2	87
149689	SRDL	24/06/2015	20/12/2015	537	179	12746	70.8 $\pm$ 34.6	75
Mean $\pm$ SD				655 $\pm$ 429	174 $\pm$ 52	8577 $\pm$ 2842	49.1 $\pm$ 9.8	85 $\pm$ 17

To assess the effect of horizontal physical gradients on the foraging behaviour of leatherback turtles (associated with HRT areas), we extracted at each turtle location the associated SST and SSH from the *Global sea physical analysis and forecast* product (PHYS 001–024) at a resolution of 0.08 ° (from U.E Copernicus Marine Service Information). We then calculated the values of SST gradient (SSTgrad) and SSH gradient (SSHgrad) at the locations of each turtle. We then used the areas with the highest SSTgrad and SSHgrad magnitude ( $\geq$  quantile 0.95) to identify the locations of oceanic fronts. Then we assessed the use of frontal zones by leatherback turtles based on the distance to the closest frontal zone identified. We repeated the analysis to determine whether the turtles directly targeted SST fronts or if they were attracted by another oceanographic feature present at frontal regions. This procedure used *Finite-Size Lyapunov Exponents* (FSLE, D'Ovidio et al., 2004) and focused on pure transport diagnostics. The FSLE method provides a direct measurement of local stirring by sub-mesoscale currents, and the separation of waters coming from different regions by the FSLE ridges makes it possible to identify water masses with different physical properties (D'Ovidio et al., 2010; De Monte et al., 2012). FSLE diagnostics were computed as described in Bon et al. (2015) and the FSLE diagnostics were extracted at each turtle location at a 0.08 ° horizontal resolution. For the SST and SSH fronts, the distance to the closest FSLE filament with a gradient magnitude  $\geq$  quantile 0.95 was then calculated for each turtle location.

### 2.7.2. Vertical variables

We assessed the habitat use of leatherback turtles in the vertical dimension by extracting sea water temperature, sea water salinity, mixed layer depth (MLD) and sea water chlorophyll *a* concentration from Copernicus Marine Service Information. These parameters were extracted at each dive location and for each maximum depth reached by all turtles equipped in 2015. The use of vertical habitat by the turtle equipped in 2014 could not be characterized due to the coarse resolution of the diving data (only 1 maximum dive depth per location). We extracted temperature, salinity and MLD (using Kara et al.'s method (2000a)) data from June 2015 to April in 2016 from the *Global physical analysis and coupled system forecast* product (PHY 001–015), available from Copernicus, at a 0.25 ° horizontal resolution and depths of 0–400 m. Similarly, we extracted sea water chlorophyll *a* concentration data from the BIO 001–014 product at a 0.5 ° horizontal resolution and depths of 0–400 m. We then used these data to locate the thermocline, halocline and nutricline depths. The seasonal thermocline was defined as the layer comprised between the MLD (upper layer of the thermocline) and the maximum MLD during the previous winter peak below (e.g. lower layer, in February 2015 for the tags deployed in June 2015). We also estimated the halocline and nutricline depths of each dive location from the salinity and chlorophyll *a* gradients, respectively.

### 2.8. Diving behaviour analysis

An indication of dive shape was obtained through the Time of Allocation at Depth (TAD) index, calculated by using the four inflection points of the summarized profiles provided by SRDL tags deployed in 2015. We used Fedak et al.'s method (2001) to calculate the TAD and thus estimate the type of activity the turtles displayed during the dives. Exploratory dives commonly corresponded to V-shaped dives with  $0.5 \leq \text{TAD} < 0.75$ , and foraging activity at the bottom of the dive corresponded to U-shaped dives with  $0.75 \leq \text{TAD} < 1$ . We fixed the average rate of change of depth at  $1.4 \text{ m s}^{-1}$ , as values above this speed are considered biologically unreliable.

## 3. Results

### 3.1. Migratory routes and high residence time (HRT) areas

The tracked turtles measured (mean  $\pm$  SD) 160  $\pm$  8.1 cm in curved carapace length, 116  $\pm$  6.4 cm in curved carapace width and 206  $\pm$  13.7 cm in circumference. We obtained 655  $\pm$  429 (mean  $\pm$  SD) locations per turtle, for a tracking duration ranging from 99 (#149680) to 281 days (#149688, Table 1). The total distance travelled varied from 4957 km (#149680) to 12746 km (#149689, mean  $\pm$  SD: 8577  $\pm$  2842 km). The actual daily speed (corrected for oceanic currents) ranged from 39.2  $\pm$  21.2 to 70.8  $\pm$  34.6 km d<sup>-1</sup> (#149688 vs. #149689, respectively, mean  $\pm$  SD: 49.1  $\pm$  9.8 km d<sup>-1</sup>). The average elapsed time to reach the HRT areas (putative foraging grounds) was 85  $\pm$  17 d (mean  $\pm$  SD; range: 65–115 d, #149680 vs. #149684, respectively).

The 10 females tracked in this study left French Guiana between late June and late August, and occupied HRT areas between August and November. They headed in various directions towards mid-latitude areas, i.e. south-eastern US continental shelf, Newfoundland-Labrador, the Azores or even pelagic waters in the North Atlantic (Fig. 1a). The areas that were identified as putative foraging grounds based on a HRT were spread between 30–45 °N, and were located either in neritic or pelagic zones. Three turtles used a coastal HRT area located off the shores of the south-eastern US shelf (#149680, #149682 and #149689). Another (#149687) remained in the neritic HRT area of Newfoundland-Labrador, at the mouth of the Saint Lawrence River, and the six remaining turtles spent most of their time in pelagic waters. The running circle providing the best contrast in terms of residence time series analysis had a radius of 80 km. The largest HRT percentage was observed from October ( $n=10$ ) to December ( $n=8$ ) (Fig. 1b).

### 3.2. Associations with biological features

The initial part of the migration within the core of the North Atlantic subtropical gyre corresponded to low RT (hereafter 'transit

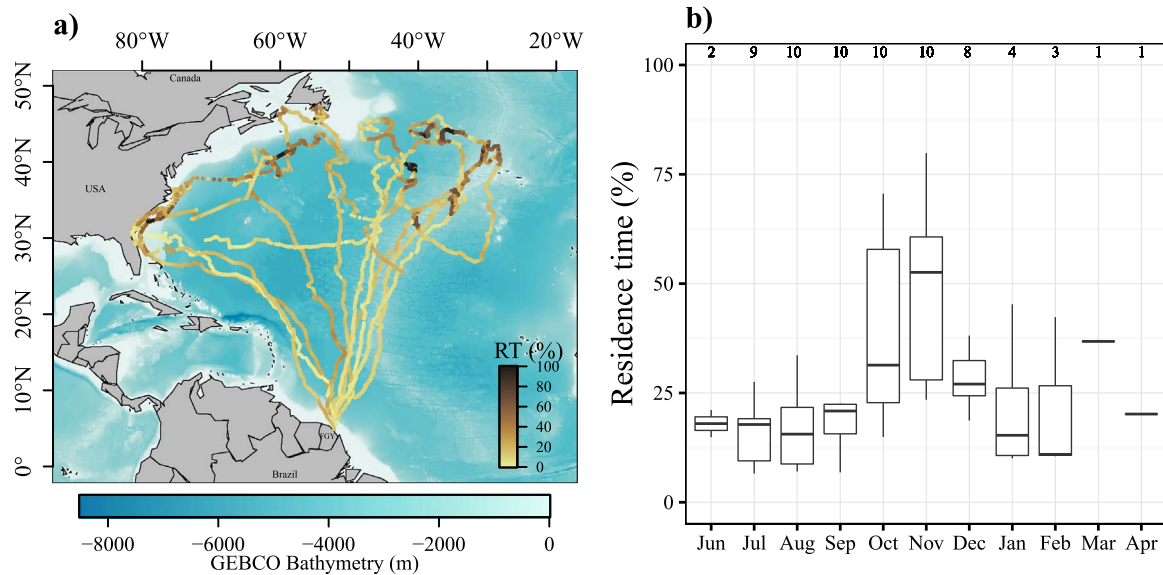


**Fig. 1.** (a) Proportion of residence time (RT in %) calculated along the 10 leatherback tracks in 2014 ( $n=1$ ) and 2015 ( $n=9$ ) and (b) box plots of RT (in %) according to the months of tracking. The RT (initially expressed in days) was converted into a percentage based on the maximum value obtained for each individual to obtain a comparable scale across individuals. (b) The locations associated with the highest values in (a) were considered to be potential foraging areas. FGY indicates the departure point and tagging site located in French Guiana. The numbers in (b) refer to the sample size of each box plot (i.e. the number of turtles; note that only one turtle was still tracked in March and April).

phase') for all females in scantily productive waters containing low levels of micronekton biomass and chlorophyll *a* concentration (Figs. 2a and 2d). When all the transit phases were taken into account, the micronekton biomass was significantly lower than that found in HRT areas (mean  $\pm$  SE:  $0.56 \pm 0.04$  vs.  $1.31 \pm 0.25$  g m<sup>-2</sup>, respectively, Wilcoxon test,  $V=35$ ,  $p < 0.05$ , Fig. 3a). Similarly, the chlorophyll *a* concentration was significantly lower at locations where the turtles transited (mean  $\pm$  SE:  $0.18 \pm 0.04$  vs.  $0.53 \pm 0.13$  mg m<sup>-3</sup>, respectively, Wilcoxon test,  $V=28$ ,  $p < 0.05$ , Fig. 3b).

Locations at higher latitudes ( $> 30^\circ$  N) correspond to areas where the turtles spent most of their migration time, and highly productive waters for both the micronekton biomass and the chlorophyll *a* were recorded (Figs. 2b, 2e and 5b). However, most of the leatherback turtles headed southward on leaving these mid-latitude feeding grounds, remaining in waters of expected high chlorophyll *a* concentration (Fig. 2f) rather than high micronekton biomass (Fig. 2c). The euphotic depth was significantly shallower in HRT areas (mean  $\pm$  SE:  $77.9 \pm 3.3$  vs.  $55.5 \pm 4.8$  m; Wilcoxon test,  $V=36$ ,  $p < 0.005$ ) – see Figs. 3c, 2g, 2h, 2i. Waters of shallower euphotic depth were associated with higher latitudes ( $> 30^\circ$  N), where the turtles were assumed to feed intensively (Fig. 2h).

### 3.3. Associations with physical discontinuities

Our turtles experienced warm waters ( $\sim 30^\circ$  C) when crossing the core of the North Atlantic subtropical gyre (see Fig. 4a). After reaching HRT areas at higher latitudes in November, they remained in cooler waters ranging mainly between 15 and 23 °C (Fig. 4b). At the beginning of winter (January), the cold waters coming from the Labrador Current extended further south and the four remaining turtles tracked at this period tended to follow the 20 °C isotherm southward (Fig. 4c). The SSH and SST were significantly lower when the turtles occupied HRT areas (mean  $\pm$  SE:  $9.4 \pm 2.8$  vs.  $-14.1 \pm 3.4$  cm; Wilcoxon test,  $V=55$ ,  $p < 0.005$ , Figs. 3g, 4d, 4e, 4f, and mean  $\pm$  SE:  $25.7 \pm 0.5$  vs.  $20.5 \pm 1.2$  °C; Wilcoxon test,  $V=55$ ,  $p < 0.005$ , Fig. 3h, respectively).

During the first and final parts of the migration, corresponding to the low RT phases, the turtles crossed waters associated with low horizontal gradients (SST and SSH fronts), as illustrated in Figs. 6a, 6c, 6d and 6f. They crossed waters associated with low FSLE (Figs. 6g and 6i). In contrast, they remained close to stronger SSH and SST gradients while occupying HRT areas at mid-latitudes (Figs. 6b and 6e). The SST

gradient was up to three times higher when on HRT areas (mean  $\pm$  SE:  $0.01 \pm 0.002$  vs.  $0.03 \pm 0.006$  °C km<sup>-1</sup>, Wilcoxon test,  $V=1$ ,  $p < 0.01$ ) – see Figs. 6a, 6b and 6c. The SSH gradient was up to twice as high when the turtles occupied HRT areas (mean  $\pm$  SE:  $0.14 \pm 0.01$  vs.  $0.25 \pm 0.05$  cm km<sup>-1</sup>, Wilcoxon test,  $V=1$ ,  $p < 0.05$ ) – see Figs. 6d, 6e and 6f. The distance to the SST front was significantly shorter when the turtles were in HRT areas than when they were on low RT areas (mean  $\pm$  SE:  $379 \pm 32$  vs.  $37 \pm 7.5$  km; Wilcoxon test,  $V=55$ ,  $p < 0.005$ ) – see Figs. 3d and 5c. Similarly, the distance to the SSH front was significantly shorter when the turtles were in HRT areas (mean  $\pm$  SE:  $474 \pm 44$  vs.  $86 \pm 22$  km, Wilcoxon test,  $V=55$ ,  $p < 0.005$ ) – see Figs. 3e and 5d). However, the FSLE was not significantly higher when the turtles occupied HRT areas (mean  $\pm$  SE:  $0.13 \pm 0.02$  vs.  $0.21 \pm 0.05$  days<sup>-1</sup>, Wilcoxon test,  $V=4$ ,  $p=0.1094$ ) – see Figs. 6g, 6h and 6i. The distance to the FSLE (filaments) was significantly shorter when the turtles were in HRT areas (mean  $\pm$  SE:  $253 \pm 34$  vs.  $64 \pm 22$  km; Wilcoxon test,  $V=54$ ,  $p < 0.005$ ) – see Figs. 3f and 5e.

### 3.4. Diving behaviour and vertical structures

#### 3.4.1. Turtle maximum depth and dive duration

The Argos-GPS tag recorded 4539 depths and 4614 dive durations. Among the 720 summarized dives transmitted (the tags have not recorded the dives continuously) by the 9 SRDL, on average  $80 \pm 33$  dives per individual were transmitted (range: 41–137 dives per turtle, #149680 vs. 149688). Over the 10 tags, 27% of the dives were less than 10 m deep (Fig. 7a). Maximum dive depths were significantly different between individuals (Kruskal-Wallis rank sum test,  $\chi^2=49$ ,  $p < 0.001$ ). The turtles dove significantly deeper when occupying low RT areas (mean  $\pm$  SE:  $82.4 \pm 5.6$  vs.  $38.5 \pm 7.9$  m, Wilcoxon test,  $V=55$ ,  $p < 0.005$ ) – see Fig. 7a. Dive durations varied from 0.5 to 85 min, with 26% of the dives lasting less than 10 min, and 31% between 20 and 45 min (Fig. 7b). Dive durations differed significantly between individuals (Kruskal-Wallis rank sum test,  $\chi^2=57$ ,  $p < 0.001$ ). The turtles performed longer dives when in low RT areas (mean  $\pm$  SE:  $27.0 \pm 1.3$  vs.  $14.3 \pm 2.4$  min, Wilcoxon test,  $V=54$ ,  $p < 0.005$ ) – see Fig. 7b.

#### 3.4.2. Surface interval and TAD

Among the 720 dives recorded by the SRDL tags, 76% of the surface intervals lasted less than 5 min (mean  $\pm$  SE:  $13.1 \pm 2.4$  min). Surface

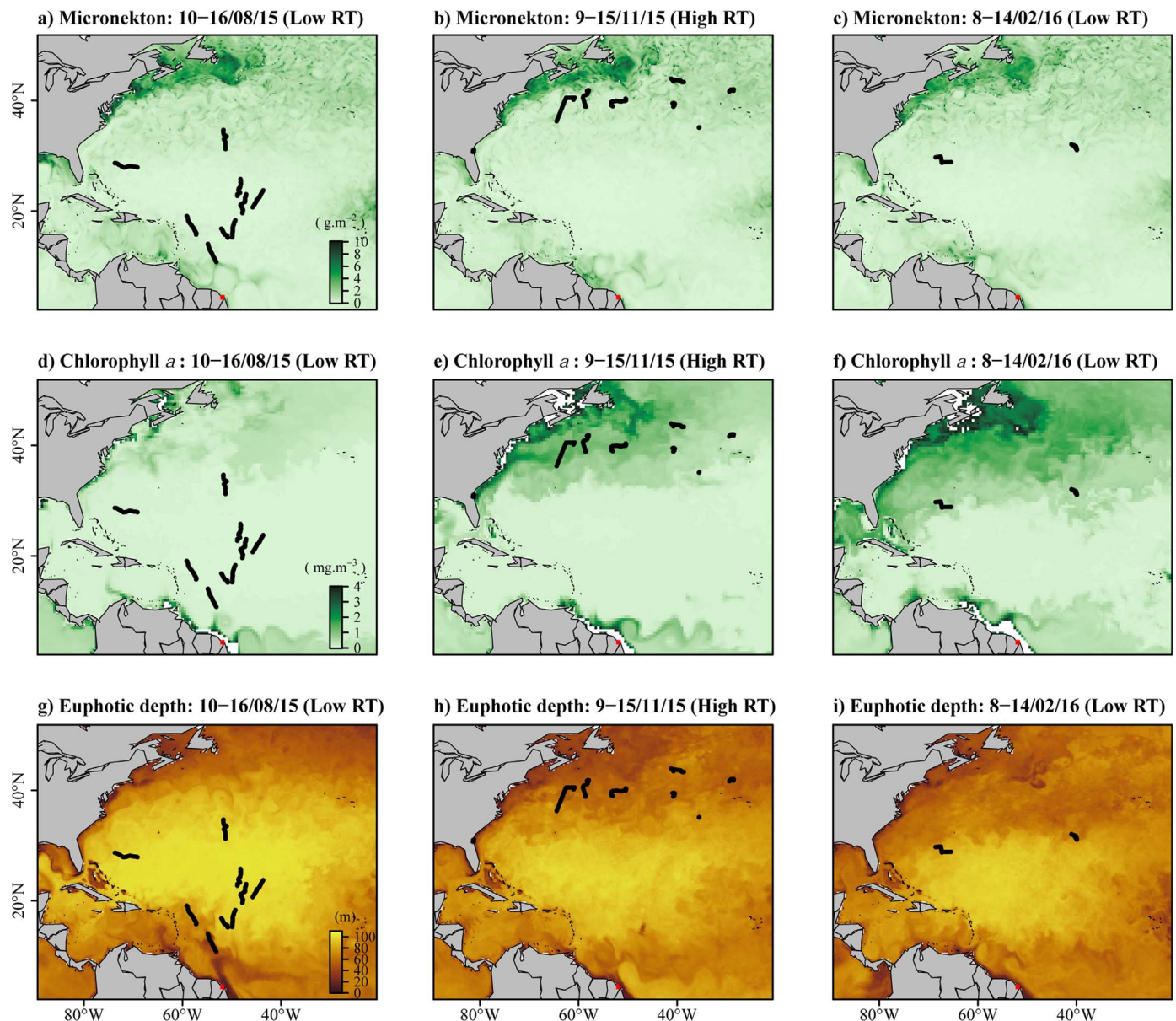


**Fig. 2.** Maps of the weekly averaged micronekton biomass predicted by SEAPODYM (a, b, c), the chlorophyll *a* concentration extracted from Copernicus (d, e, f) and the euphotic depth (g, h, i) predicted by SEAPODYM during three phases: the crossing of the North Atlantic gyre (a, d, g: low RT,  $n=10$ ), the high RT period at mid-latitudes (b, e, h,  $n=10$ ) and after leaving the high RT areas (c, f, i,  $n=3$ ). The black dots correspond to the locations of the leatherback turtles tracked from French Guiana for the corresponding week and the red square to the migration starting point. (For interpretation of the references to color in this figure legend, the reader is referred to the web version of this article.)

intervals recorded by the 9 SRDL tags differed significantly between individuals (Kruskal-Wallis rank sum test,  $\chi^2=68$ ,  $p < 0.001$ ) but did not differ significantly according to the type of behaviour (mean  $\pm$  SE:  $12.9 \pm 2.6$  vs.  $11.3 \pm 2.6$  min, Wilcoxon test,  $V=18$ ,  $p=0.6523$ ). The Time of Allocation at Depth (TAD) varied from 0.25 to 0.92 and was on average ( $\pm$  SE)  $0.59 \pm 0.004$ . With a TAD below 0.5, 11% of the 720 dives recorded by the SRDL tags could not be assigned to a U or V dive shape, whereas 85% corresponded to V-shaped dives and 4% to U-shaped dives.

#### 3.4.3. SST and temperature at turtle maximum depth

The values for SST and temperature at the maximum recorded depth of each turtle decreased over the tracking period, with the highest values recorded during the first month of tracking in June (mean  $\pm$  SE:  $28.1 \pm 0.3$  and  $27.6 \pm 0.1$  °C, SST and temperature at maximum dive depth respectively) and the lowest in November (mean  $\pm$  SE:  $21.1 \pm 3.1$  and  $20.7 \pm 3.1$  °C) – see Fig. 8. The difference between SST and temperature at maximum depth varied between 0 to 6.2 °C, and was at its highest in July (mean  $\pm$  SE:  $3.6 \pm 1.4$  °C) and lowest in February ( $0.09 \pm 0.1$  °C). This

smaller difference between SST and temperature at maximum depth coincides with the strong deepening of the mixed layer from October to February (Fig. 8).

#### 3.4.4. Mixed layer depth and thermocline

The deepness of the mixed layer at turtles' locations increased substantially between August and November (mean  $\pm$  SE:  $31.6 \pm 10.7$  vs.  $96.1 \pm 49.7$  m) – see Figs. 8 and 9. The lower limit of the thermocline also deepened from June (9.4 m,  $n=2$ ) to November (mean  $\pm$  SE:  $260.3 \pm 121.7$  m,  $n=8$ ), then became slightly shallower (February mean  $\pm$  SE:  $175.5 \pm 43.3$  m,  $n=3$ ). The turtles remained above it while occupying HRT areas (from October). Before reaching HRT areas (June to October), the turtles dived mainly below the mixed layer (Fig. 9). Afterwards, they performed shallower dives from October to February, remaining within the mixed layer (Fig. 9).

#### 3.4.5. Nutricline and halocline

Turtle maximum dive depth was positively correlated to the vertical

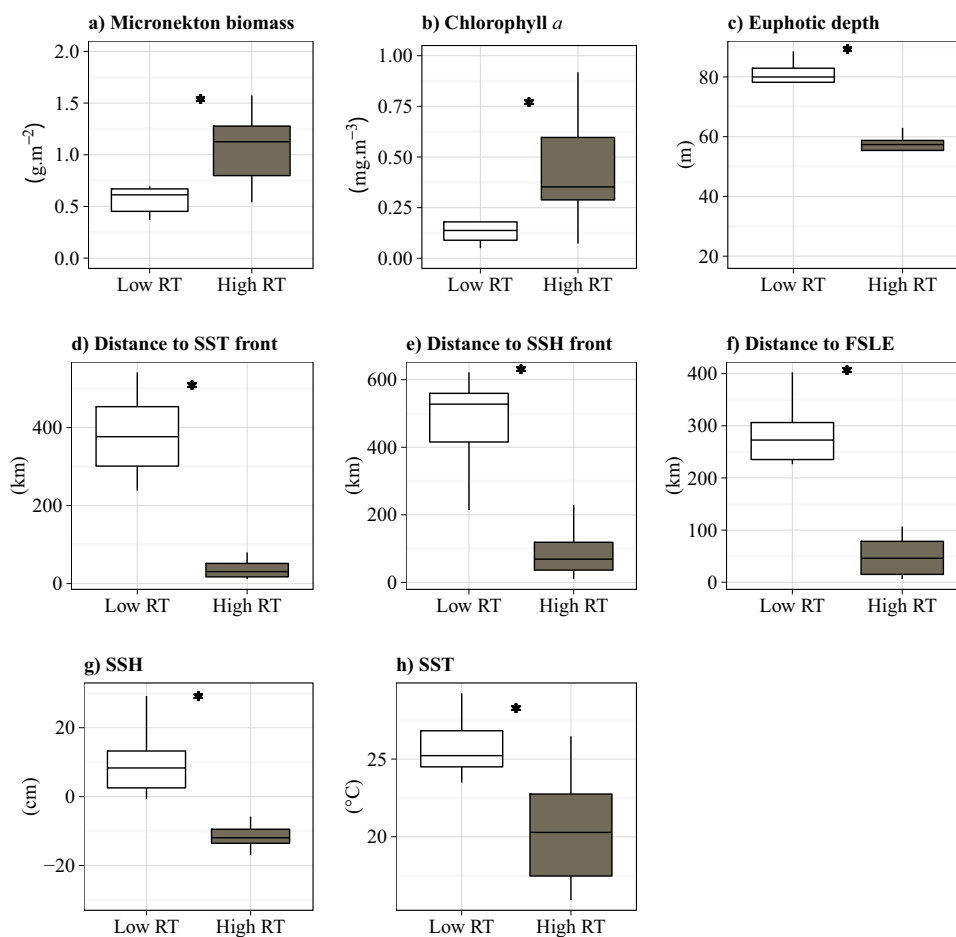


**Fig. 3.** Box plots of micronekton biomass (a), chlorophyll *a* concentration (b), euphotic depth (c), distance to the closest SST front (d), distance to the closest SSH front (e), distance to the closest FSLE filament (f), SSH (g) and SST (h) for both modes (low RT in white and high RT in dark grey). The stars in each plot indicate the significant differences between the two modes for each variable.

chlorophyll *a* gradient magnitude (nutricline depth derived from model forecast, Spearman correlation test:  $R^2=0.34$ ,  $p < 0.001$ ) and to the depth at which chlorophyll *a* concentration is maximum (Spearman correlation test:  $R^2=0.41$ ,  $p < 0.001$ ). However, the maximum dive depth reached by the leatherback was not correlated to the magnitude of the vertical salinity gradient (halocline depth derived from model forecast, Spearman correlation test:  $R^2=-0.015$ ,  $p=0.682$ ).

#### 4. Discussion

The use of satellite tracking together with a set of environmental variables (from remote sensing data and model simulations) in this study allowed us to shed light on the role played by the Gulf Stream frontal system in the selection of areas eliciting high residence times (HRT) by the North Atlantic leatherback turtle.

##### 4.1. Migration across the North Atlantic basin

The movement and diving behaviours of the leatherback turtle have been comprehensively investigated on an international scale over the past decade, with particular attention paid to their migration cycle across the Atlantic Ocean (Bailey et al., 2012b; Eckert et al., 2006b; Fossette et al., 2010b, 2010a; James et al., 2005a, 2005b; Ferraroli et al., 2004; Hays et al., 2004; McMahon and Hays, 2006; López-Mendilaharsu et al., 2009; Dodge et al., 2014). Although numerous studies have been conducted in populations from western French Guiana (Fossette et al., 2008, 2010b, 2010a), the present study is the first to investigate the movements and diving behaviour of individuals

from the Eastern population. Despite the genetic differences between the two French Guianese populations (Molfetti et al., 2013), the eastern and western individuals showed similar movement patterns. Indeed, like adult females from the Western population (see Fossette et al., 2010b, 2010a; Ferraroli et al., 2004), our tracked individuals migrated northward to reach relatively higher latitudes ( $> 30^\circ \text{N}$ ) where they tended to display movement behaviour leading to a local increase in residence time during autumn and winter, in either coastal or pelagic habitats. The HRT spent in some particular areas at mid-latitudes indicate that these areas may correspond to foraging grounds. The importance of these potential foraging grounds for this species is reinforced by previous studies that have already reported same hot-spots for the leatherback in Florida, Nova Scotia and the Azores (Eckert et al., 2006b; Fossette et al., 2010a, 2010b; Ferraroli et al., 2004; James et al., 2006; Hamelin et al., 2014). After occupying HRT areas at mid-latitudes, the two turtles that transmitted data for the longest tracking durations headed back southward. While in high RT areas, these two individuals have experienced low SST reaching up to  $12^\circ \text{C}$ . Despite these occasional SST encountered, for most of our tracked turtles, the thermal barrier seemed to occur between the  $15\text{--}20^\circ \text{C}$  SST isotherm while foraging, with 77% of the turtles remaining in warmer water than  $15^\circ \text{C}$ . These findings are in accordance with the  $15^\circ \text{C}$  thermal tolerance suggested by McMahon and Hays (2006) for this species. Indeed, despite their endothermic capacity (James and Mrosovsky, 2004), it has been suggested that temperature thresholds might limit the amount of time the leatherback turtles can spend in some cold water areas (Witt et al., 2007). The relatively short tag life ( $6 \pm 2$  months) was however a drawback for this study, which would



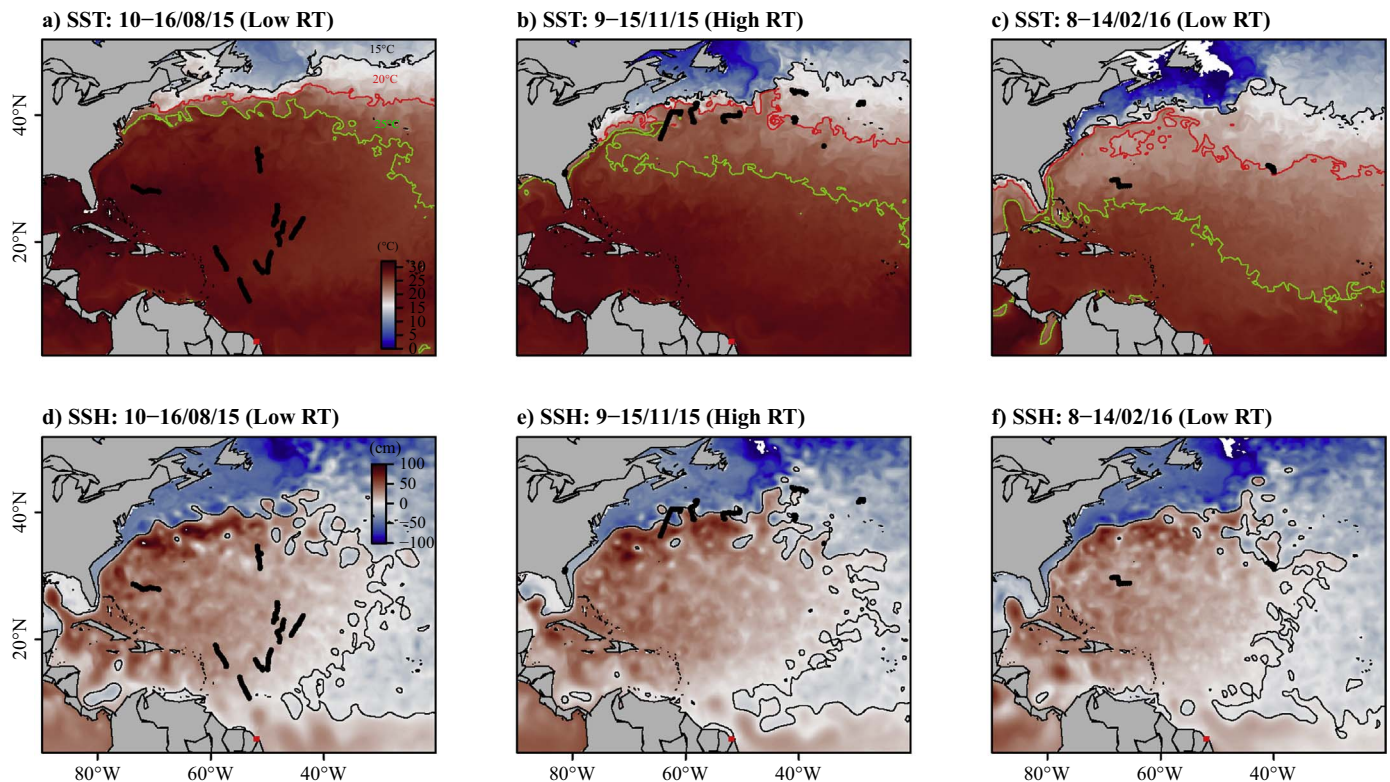


**Fig. 4.** Maps of the weekly averaged SST (a, b, c) and SSH (d, e, f) derived from Copernicus during three phases: the crossing of the North Atlantic gyre (a, d: low RT,  $n=10$ ), the high RT period at mid-latitudes (b, e,  $n=10$ ) and after leaving the high RT areas (c, f,  $n=3$ ). Three SST contours were superimposed: 15 °C, 20 °C and 25 °C, and the SSH contour (0 cm) refers to the location of the Gulf Stream front. The black dots correspond to the locations of the leatherback turtles tracked from French Guiana for the corresponding week and the red square to the migration starting point. (For interpretation of the references to color in this figure legend, the reader is referred to the web version of this article.)

require a period of 2–4 years to track the entire remigration cycle across the North Atlantic Basin. There is thus a clear need for further tag deployment to identify the different habitats targeted by this species during post-nesting migration.

#### 4.2. Associations with biological variables

In this study, the leatherback turtles travelled at high speed when crossing the nutrient-poor North Atlantic subtropical gyre, reflecting a transit behaviour. This area is considered as an ‘ocean desert’ (Tomczak and Godfrey, 2013), due to its scant primary productivity ( $0.50 \text{ mg C m}^{-2} \text{ d}^{-1}$ , Mara $\tilde{\text{n}}\text{on et al., 2000}$ ). In contrast, the turtles spent more time and concentrated searching in HRT areas in the colder waters of upwelling and mid-latitude regions (Mara $\tilde{\text{n}}\text{on et al., 2000}$ ), where primary productivity can reach up to  $1000 \text{ mg C m}^{-2} \text{ d}^{-1}$ . There is a lack of documentation concerning the spatial distribution of jellyfish (Houghton et al., 2006), but primary production or chlorophyll  $a$  concentration were evidenced to be good proxies for leatherback prey availability (Fossette et al., 2010a; Dodge et al., 2014). The probability to forage was shown to increase with chlorophyll  $a$  concentration (up to  $2.5 \text{ mg m}^{-3}$ ) for the Western Pacific (Bailey et al., 2012b) and the North Atlantic populations (Dodge et al., 2014). Similar results were found in our study, where values of chlorophyll  $a$  on assumed foraging grounds (corresponding to HRT areas) reached concentrations up to three times higher than those recorded in transit areas ( $0.18 \pm 0.04$  vs.  $0.53 \pm 0.13 \text{ mg m}^{-3}$ , respectively). Furthermore, a clear match was observed between the high chlorophyll  $a$  concentrations and the HRTs, evidencing a remarkable synchronization of this species with areas of high productivity in the North Atlantic. However, as chlorophyll  $a$  concentrations come from forecasting ocean models (Copernicus database), we can observe some discrepancies, such as the subtropical gyres of the North Atlantic that are predicted slightly too oligotrophic, or the over-estimation of the chlorophyll  $a$  in the tropical band. Such differences may lead to misinterpretation of tracking data when looking at fine-scale

movements (1–10 s of km). But the purpose of our study was to look at mesoscale patterns (10–100 km) and consider relative chlorophyll  $a$  values (and not absolute values) to fit the accuracy of our tracking data, making the output of Copernicus model adequate and reliable.

As mentioned by Fossette et al. (2010b), a more reliable picture of jellyfish distribution may be obtained by looking at a higher trophic level than chlorophyll  $a$  (Strömberg et al., 2009). In this context, SEAPODYM recently appeared as a promising model to provide estimations of the spatio-temporal distribution of micronekton, including cephalopods, crustaceans, fishes and jellyfish (Lehodey et al., 2010). We therefore hypothesized that the micronekton biomass provided by this model would match locations of foraging leatherbacks better than chlorophyll  $a$ . Although the presence of chlorophyll  $a$  seemed to better match the occurrence of HRT areas, levels of micronekton at these locations were more than twice higher than those found in low RT areas ( $0.55 \pm 0.04$  vs.  $1.31 \pm 0.25 \text{ g m}^{-2}$ ). SEAPODYM predictions were based on the maturation time of pelagic organisms, i.e. 1–2 months for zooplankton and 10 months for micronekton (both at 15 °C; Conchon, unpublished data), but the maturation time of jellyfish is shorter than 10 months. This may explain why the concentration of micronekton biomass was not at its highest in HRT areas at mid-latitudes. A further study including the zooplankton output updated from SEAPODYM may nevertheless provide a better explanation for the habitat selection by leatherbacks.

#### 4.3. Associations with physical discontinuities

The Eastern French Guianese leatherback turtles we tracked tended to display HRT behaviour mainly along physical discontinuities at mid-latitudes ( $> 30^\circ \text{N}$ ), probably because such interfaces correspond to nutrient-rich waters where jellyfish aggregate (Sims and Quayle, 1998; Greer et al., 2013; Powell and Ohman, 2015). At the northern edge of the Gulf Stream, its warm waters meet the cold Labrador Current

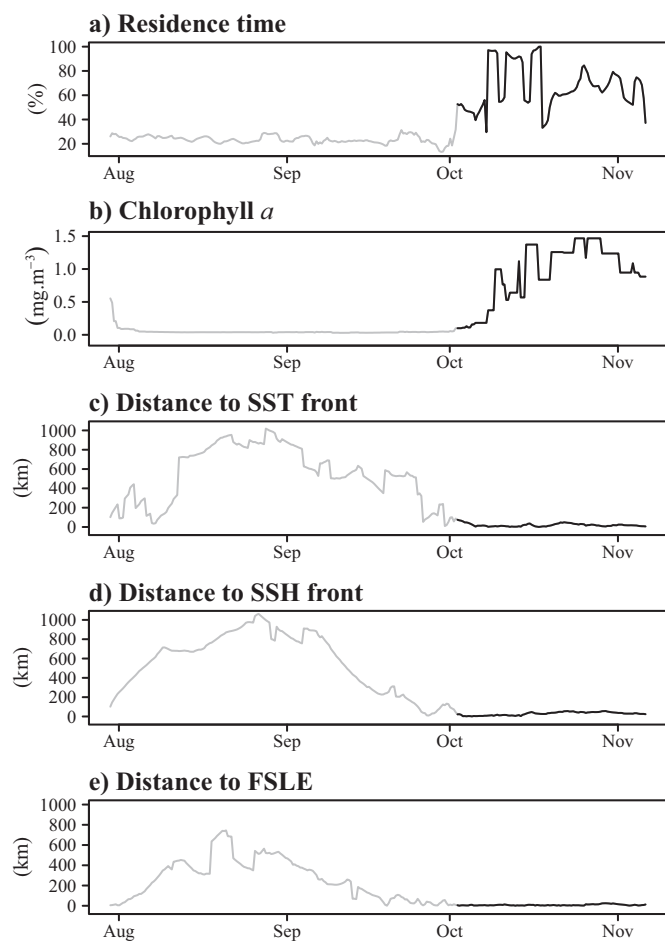


**Fig. 5.** Proportion of RT (a, in %) and four environmental variables (b, c, d, e) extracted along the track of turtle #149680, namely: chlorophyll *a* concentration (b), distance to the closest SST front (c), distance to the closest SSH front (d) and distance to the closest FSLE filament (e). The highest RT values (from October onwards) were considered to be a foraging activity, and the black parts of the lines refer to the putative foraging mode.

waters, creating a sharp temperature gradient in an area referred as the Gulf Stream north wall (GSNW, Sanchez-Franks et al., 2015). The shelf-slope front (SSF), a front located off the northeast coast of the United States and Canada, separates colder, less saline continental shelf waters from warmer and more saline slope waters (Bisagni et al., 2009), where most of our turtles (60%) displayed HRT behaviour. However, the HRT areas of three turtles were located on the shelf waters south of North Carolina–United States, in the South Atlantic Bight, where they used the lower branch of the Gulf Stream, characterized by much less extreme temperature gradients. Our results highlighted a surprising synchronization and aggregation of all the leatherback turtles between these two fronts before migrating back south.

HRT areas tended to occur preferentially along the SST and SSH gradients, as well as along the FSLE filaments. The identification of these frontal zones enabled us to delineate the frontal boundaries of the GSNW and the SSF. The strong association with these physical discontinuities was confirmed by the shorter distance to the closest front (SST gradient, SSH gradient and FSLE filament) while in HRT areas compared to transit periods. Several studies have already described the tendency for some sea turtles species (loggerhead and leatherback) to associate with frontal structures in the Pacific with the Kuroshio Current (Polovina et al., 2004, 2006; Polovina and Howell, 2005; Scales et al., 2015), or in Atlantic Ocean with the Gulf Stream (Eckert et al., 2006b; Fossette et al., 2010a; Lutcavage, 1996; Witherington, 2002). But to date, only one study has demonstrated such affinities between the leatherback movements and the Gulf Stream

frontal system using oceanographic data (Dodge et al., 2014), but such findings were limited to the horizontal dimension and true for a limited number of individuals ( $n=2$ ). The associations with filaments at the sub-mesoscale in our study (identified via FSLE), in agreement with findings in previous studies conducted on penguins (Lowther et al., 2014; Bon et al., 2015; Whitehead et al., 2016) and seals (Nordstrom et al., 2013; Lowther et al., 2014), confirms the importance of frontal areas in the aggregation of prey.

Regions of high FSLE and strong SSH and SST gradients may all provide complementary data facilitating the interpretation of animal tracking (De Monte et al., 2012). Strong SSH gradients correspond to high kinetic energy and high FSLE to confluence/frontal regions, while a strong SST gradient corresponds to frontal regions marked by temperature difference, where upwelling/downwelling can occur. These three diagnostics can diverge in regions of intermediate or weak kinetic energy, where a confluence is the result of the interaction of multiple mesoscale features and of their temporal evolution and in which high SST gradients only occur at certain confluences (D'Ovidio et al., 2013). However, these diagnostics may be strongly correlated in highly energetic and contrasted regions where gradient intensification by the mesoscale currents arises on relative short time scales (i.e. days), and coincide with the occurrence of strong temperature gradients. This is the case for the branch of the Gulf Stream targeted by the turtles in our study, and may explain why the associations with frontal areas are similar in terms of SST gradients, FSLE, and SSH contours.

#### 4.4. Affinities for vertical structures

The leatherback turtles we tracked performed shallower dives while in HRT areas ( $38.5 \pm 7.9$  m) than during transit ( $82.4 \pm 5.6$  m). This is in accordance with the behaviour of individuals of the Western French Guianese population ( $53.6 \pm 33.1$  vs.  $81.8 \pm 56.2$  m, Fossette et al., 2010a). This behaviour should enable them to get an easier access to prey, which is assumed to concentrate in the upper layer (Hays et al., 2008). The analysis of residence time data showed that the tracked females started to display HRT behaviour during early autumn (October), when the phytoplankton bloom begins along the GSNW (Friedland et al., 2016) and the phytoplankton net growth rate increases in the subarctic Atlantic waters located further north ( $> 40$  °N, Behrenfeld, 2010). We equipped our turtles at the nesting peak in June to obtain a reliable picture of the population trend. Despite the low light conditions in the North Atlantic during autumn and winter, the deep winter mixing of the upper layer favours the phytoplankton bloom formation via biomass accumulation (Behrenfeld, 2010). During low stratification months (October–May) in the South Atlantic Bight, where three turtles spent most of their time, the winds and small temperature differences between nutrient-rich water intrusions and the overlaying cold waters bring subsurface nutrient intrusions to the upper layers, as well as cold air outbreaks, favouring the frequent vertical redistribution of chlorophyll *a* and therefore avoiding nutrient depletion in this region (Martins and Pelegrí, 2006).

As our turtles performed mostly shallow dives while in HRT areas at mid-latitudes, the depths they reached during this period were mainly within the mixed layer. In the North Atlantic, the deepest mixed layer occurs between January and May during deep water formation at  $\sim 40$  °N (Kara et al., 2003). The mixed layer started deepening in October at locations further south ( $30$ – $40$  °N) where the turtles aggregated, coinciding with the period when the turtles started performing shallower dives. The turtles remained within this mixed layer while in HRT areas over the winter period ( $n=4$  in January to  $n=1$  in April). A similar behaviour was observed by Fossette et al. (2010a) for the Eastern French Guianese leatherback turtles, and could be performed to get an easier access to their prey by maximizing energy gain while foraging. Reaching shallower depths while in HRT areas may also reflect the distribution of jellyfish, which is known to be more abundant in the upper layer in cold waters (Longhurst et al., 1995).

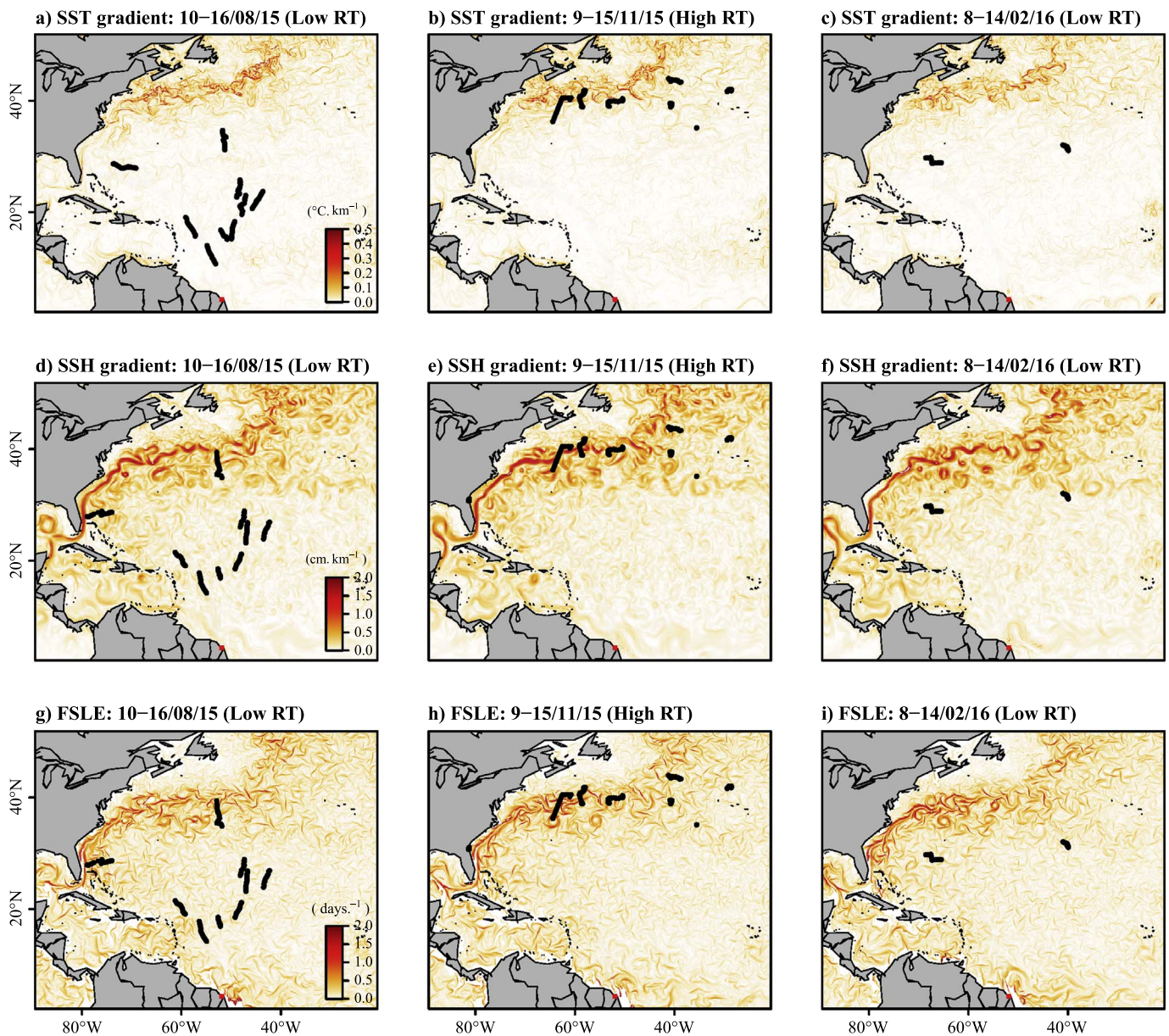


**Fig. 6.** Maps of the weekly averaged SST gradient (a, b, c), SSH gradient (d, e, f) and FSLE (g, h, i) during three phases: the crossing of the North Atlantic gyre (a, d, g: low RT,  $n=10$ ), the high RT period at mid-latitudes (b, e, h,  $n=10$ ) and after leaving the high RT areas (c, f, i,  $n=3$ ). The black dots correspond to the locations of the leatherback turtles tracked from French Guiana for the corresponding week and the red square to the migration starting point. (For interpretation of the references to color in this figure legend, the reader is referred to the web version of this article.)

This deep mixed layer, associated with high nutrient biomass, may therefore explain the remarkable aggregation of leatherback turtles at higher latitudes during autumn and winter. Although the deepest mixed layer commonly occurs during winter, it occurs during the austral autumn in the southern hemisphere in the Western Australia and coincides with high values of chlorophyll *a* (Rousseaux et al., 2012), thus enabling the replenishment of the surface waters via vertical mixing. The turtles in our study remained within the mixed layer while in HRT areas (i.e. above the upper limit of the thermocline) and dove below it while in other areas, and did not show any particular association with the thermocline or any other strong vertical gradient area (halocline or nutricline), contrary to findings in previous studies conducted on fur seals (Nordstrom et al., 2013), Atlantic olive ridleys (Chambault et al., 2016) and Atlantic leatherback turtles (Bailey et al., 2012a; Hamelin et al., 2014). This difference may be explained by the methodology used to calculate the vertical gradients: the thermocline is commonly defined based on the temperature gradient magnitude

(Bailey et al., 2012a), but this approach can be biased by incomplete temperature profiles (over the continental shelf) or insufficient depths reached by the individuals. To avoid a possibly biased identification of the thermocline depth, we decided to use the MLD provided by Copernicus as the upper limit, and the deepest mixed layer during the previous winter peak for the lower limit. In contrast, Hamelin et al. (2014) used *in situ* temperatures provided by CTD tags to determine the thermocline, which probably resulted in less errors and a better resolution than when using the outputs from ocean forecasts such as Copernicus.

In the North Atlantic, the breakdown of the seasonal thermocline under the effects of storms and winds during autumn leads to deep mixed layer that generates a quasi-uniform layer of temperature (isothermal layer) throughout the water column, with relatively homogeneous values between the upper layer of the thermocline and the surface (Lentz et al., 2003). Unlike the cooler SST encountered when performing HRT behaviour ( $20.0 \pm 3.9$  °C, range: 15.9–26.3 °C), the

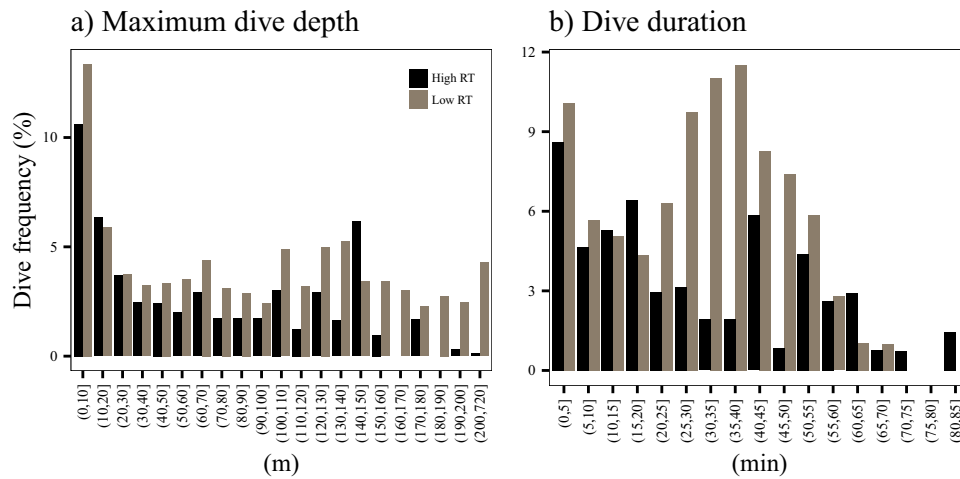


Fig. 7. Histograms of the maximum dive depth (a) and the dive duration (b) for the 10 tags deployed in 2014 ( $n=1$ ) and 2015 ( $n=9$ ) and for both modes (low RT in grey vs. high RT in black).

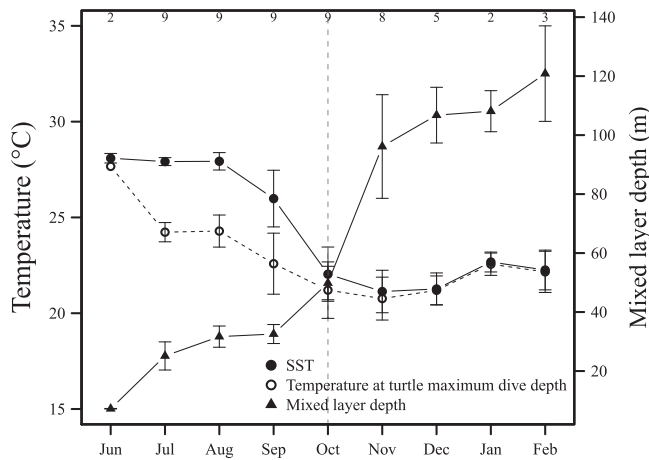


Fig. 8. Monthly mean ( $\pm$  SE) of SST (filled dots), *in situ* temperature at the turtle maximum dive depth (empty dots) and mixed layer depth (triangles) extracted for the 9 SRDL tags and from Copernicus database. The vertical dotted line refers to the beginning of the high RT period for the majority of the turtles. The numbers refer to the sample size of each box plot (i.e. the number of turtles).

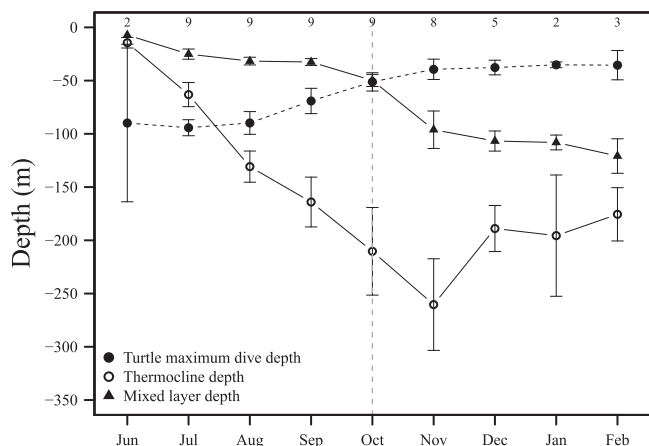


Fig. 9. Monthly mean ( $\pm$  SE) of turtle maximum dive depth (filled dots), lower limit of the thermocline (empty dots) and mixed layer depth (triangles) extracted for the 9 SRDL tags. The lower limit of the thermocline and the mixed layer depth were extracted from the Copernicus database. The vertical dotted line refers to the beginning of the high RT period for the majority of the turtles. The numbers refer to the sample size of each box plot (i.e. the number of turtles).

turtles experienced warm SST during their transit across the subtropical gyre ( $28.1 \pm 1.8$  °C, range: 20.9–30.9 °C). Besides the SST difference between the two movement modes, there was also a significant temperature difference of up to 4.2 °C between the surface and the maximum dive depth within the gyre. While crossing the gyre, the females therefore experienced shallow mixed layer and warm temperatures. As Fossette et al. (2010a) found for the western French Guianese population, our eastern French Guianese turtles performed deep dives ( $104 \pm 80.7$  m) in this nutrient-poor area (Marañón et al., 2000; Strömberg et al., 2009), which may indicate that they targeted cooler temperatures in deeper layers to save energy during the transit phase of their migration. The selection by these turtles of HRT areas located at mid-latitudes suggests a preference for cool waters (mean temperature at maximum depth:  $19.1 \pm 4.9$  °C), as observed in leatherbacks from the East Pacific population (Bailey et al., 2012b). The long post-dive surface intervals ( $13.1 \pm 2.4$  min) observed in our study reinforce the hypothesis that some individuals may swim at the surface to process and eat large prey items in the Northwest Atlantic (James and Mrosovsky, 2004). The deployment of 3D-acceleration data loggers together with cameras should make it possible to identify prey catch attempts during the dives, and therefore relate this activity to leatherback diving behaviour. Despite the relatively low number of dives recorded by the 9 SRDL tags ( $n=720$ ), the 4614 dives collected by the Argos-GPS tag provide complementary dive data to support the first evidence of the use of the mixed layer by the adult female leatherback turtles during post-nesting migration across the North Atlantic. While in high RT areas, the shallower diving behaviour of the turtles (within the first 55 m) was already evidenced by a previous study (Fossette et al., 2010b), which therefore reinforces the observed pattern of the turtles remaining mainly within the deep mixed layer. In a lesser extent, the low number of dives recorded could however prevent from observing some occasional deep dives performed below the mixed layer. To cope with this limitation, some additional SRDL tags programmed to collect several daily profiles need to be further deployed. The deployment of additional tags over longer periods (at least one year) is required to collect complementary data on both the horizontal and vertical movements, since leatherback behaviour shows inter-annual variability.

### 5. Conclusion

The present study is the first to document the post-nesting migration movements of the Eastern French Guianese population of leatherback turtles. Our findings highlight the crucial role of the Gulf Stream front in the selection of potential foraging habitats by this species. The use of innovative

and 3D ocean models for estimating SSH, temperature, salinity, chlorophyll *a*, FSLE (computed from satellite-derived currents), and micronekton biomass (from SEAPODYM) enabled us to investigate the link between leatherback movements and frontal structures in both the horizontal and vertical dimensions. Although the high residence time areas of the turtles were geographically remote (spread between 80–30 °W and 28–45 °N), these probable foraging grounds were all found in close proximity to the Gulf Stream frontal zone, a highly dynamic and productive physical discontinuity separating the warm and salty waters of the Gulf Stream from the cold and less-saline waters of the Labrador Current. As seen in other oceanic fronts, this extensive area is known to enhance primary production and thus aggregate low trophic level organisms such as jellyfish, which is the main food resource for leatherback turtles. In a context of climate change, anticipating the evolution of such frontal structure under the influence of global warming is crucial to ensure the conservation of this vulnerable species.

## Acknowledgments

This study was carried out within the framework of the Plan National d'Action Tortues Marines de Guyane and was produced as part of the CARET2 cooperation project between French Guiana and Suriname, headed by the French Guiana office of WWF-France, in partnership with Kwata NGO, the French National Agency for Hunting and Wildlife (ONCFS), the French Guiana Regional Nature Park (PNRG) and WWF Guianas. PC was supported by Shell and CNES Guyane (n° 475591). The authors also appreciate the support of the ANTIDOT project (Pépinière Interdisciplinaire Guyane, Mission pour l'Interdisciplinarité, CNRS), French Guiana Regional Council, the EDF Foundation and Fondation de France (n° 0047667). We also thank Anna Conchon (CLS) for her availability in transferring SEAPODYM outputs, Francesco d'Ovidio (LOCEAN) for his helpful advice regarding the FSLE diagnostics, Joël Sudre (LEGOS) for extracting the geostrophic and Ekman current data, Timothé Tartrat (IPHC) and Joffrey Jouma'a for their fruitful exchanges regarding the analyses.

## References

Acha, E.M., Mianzan, H.W., Guerrero, R.A., Favero, M., Bava, J., 2004. Marine fronts at the continental shelves of austral South America: physical and ecological processes. *J. Mar. Syst.* 44, 83–105.

Bailey, H., Benson, S.R., Shillinger, G.L., Bograd, S.J., Dutton, P.H., Eckert, S.A., Morreale, S.J., Paladino, F.V., Eguchi, T., Foley, D.G., Block, B.A., Piedra, R., Hitipeuw, C., Tapilatu, R.F., Spotila, J.R., 2012a. Identification of distinct movement patterns in Pacific leatherback turtle populations influenced by ocean conditions. *Ecol. Appl.* 22, 735–747.

Bailey, H., Fossette, S., Bograd, S.J., Shillinger, G.L., Swithenbank, A.M., Georges, J.-Y., Gaspar, P., Strömberg, K.H.P., Paladino, F.V., Spotila, J.R., Block, B.A., Hays, G.C., 2012b. Movement patterns for a critically endangered species, the leatherback turtle (*Dermodochelys coriacea*), linked to foraging success and population status. *PLOS ONE* 7, e36401.

Baillieux, F., Cotté, C., Guinet, C., 2010. Mesoscale eddies as foraging area of a deep-diving predator, the southern elephant seal. *Mar. Ecol. Prog. Ser.* 408, 251–264.

Barraquand, F., Benhamou, S., 2008. Animal movements in heterogeneous landscapes: identifying profitable places and homogeneous movement bouts. *Ecology* 89, 3336–3348.

Behrenfeld, M.J., 2010. Abandoning Sverdrup's critical depth hypothesis on phytoplankton blooms. *Ecology* 91, 977–989.

Belkin, I., Krishfield, R., Honjo, S., 2002. Decadal variability of the North Pacific Polar Front: Subsurface warming versus surface cooling. *Geophys. Res. Lett.* 29, (65–1).

Belkin, I.M., Cornillon, P.C., Sherman, K., 2009. Fronts in large marine ecosystems. *Prog. Oceanogr.* 81, 223–236.

Benhamou, S., Riotte-Lambert, L., 2012. Beyond the Utilization Distribution: identifying home range areas that are intensively exploited or repeatedly visited. *Ecol. Model.* 227, 112–116.

Bisagni, J.J., Kim, H.-S., Chaudhuri, A., 2009. Interannual variability of the shelf-slope front position between 75° and 50°W. *J. Mar. Syst.* 78, 337–350.

Block, B.A., Dewar, H., Blackwell, S.B., Williams, T.D., Prince, E.D., Farwell, C.J., Boustany, A., Teo, S.L.H., Seitz, A., Walli, A., Fudge, D., 2001. Migratory movements, depth references, and thermal biology of Atlantic Bluefin Tuna. *Science* 293, 1310–1314.

Block, B.A., Teo, S.L.H., Walli, A., Boustany, A., Stokesbury, M.J.W., Farwell, C.J., Weng, K.C., Dewar, H., Williams, T.D., 2005. Electronic tagging and population structure of Atlantic bluefin tuna. *Nature* 434, 1121–1127.

Bon, C., Della Penna, A., Ovidio, F. d., Y.P. Arnould, J., Poupart, T., Bost, C.-A., 2015. Influence of oceanographic structures on foraging strategies: macaroni penguins at Crozet Islands. *Mov. Ecol.* 3, 32.

Bradshaw, C.J.A., Hindell, M.A., Sumner, M.D., Michael, K.J., 2004. Loyalty pays: potential life history consequences of fidelity to marine foraging regions by southern elephant seals. *Anim. Behav.* 68, 1349–1360.

Brodeur, R.D., Seki, M.P., Pakhomov, E., Sunstov, A.V., 2005. Micronekton-What are they and why are they important. *Pac. Mar. Sci. Org. Press* 13, 7–11.

Chambault, P., Pinaud, D., Vantrepotte, V., Kelle, L., Entraygues, M., Guinet, C., Berzins, R., Bilo, K., Gaspar, P., Thoisy, B., de Maho, Y.L., Chevallier, D., 2015. Dispersal and diving adjustments of the green turtle *Chelonia mydas* in response to dynamic environmental conditions during post-nesting migration. *PLOS ONE* 10, e0137340.

Chambault, P., Thoisy, B. de, Heerah, K., Conchon, A., Barrioz, S., Dos Reis, V., Berzins, R., Kelle, L., Picard, B., Roquet, F., Le Maho, Y., Chevallier, D., 2016. The influence of oceanographic features on the foraging behavior of the olive ridley sea turtle *Lepidochelys olivacea* along the Guiana coast. *Prog. Oceanogr.* 142, 58–71.

Cotté, C., Park, Y.-H., Guinet, C., Bost, C.-A., 2007. Movements of foraging king penguins through marine mesoscale eddies. *Proc. R. Soc. Lond. B Biol. Sci.* 274, 2385–2391.

D'Ovidio, F., Fernández, V., Hernández-García, E., López, C., 2004. Mixing structures in the Mediterranean Sea from finite-size Lyapunov exponents. *Geophys. Res. Lett.* 31, L17203.

D'Ovidio, F., Monte, S.D., Alvain, S., Dandonneau, Y., Lévy, M., 2010. Fluid dynamical niches of phytoplankton types. *Proc. Natl. Acad. Sci.* 107, 18366–18370.

D'Ovidio, F., Monte, S.D., Penna, A.D., Cotté, C., Guinet, C., 2013. Ecological implications of eddy retention in the open ocean: a Lagrangian approach. *J. Phys. Math. Theor.* 46, 254023.

De Monte, S., Cotté, C., Ovidio, F. d., Lévy, M., Corre, M.L., Weimerskirch, H., 2012. Frigatebird behaviour at the ocean-atmosphere interface: integrating animal behaviour with multi-satellite data. *J. R. Soc. Interface* 9, 3351–3358.

Dodge, K., Galuardi, B., Miller, T.J., Lutcevage, M.E., 2014. Leatherback turtle movements, dive behavior, and habitat characteristics in ecoregions of the Northwest Atlantic Ocean. *PLOS ONE* 9, e91726.

Doniol Valcroze, T., Berteaux, D., Larouche, P., Sears, R., 2007. Influence of thermal fronts on habitat selection by four orqueal whale species in the Gulf of St. Lawrence. *Mar. Ecol. Prog. Ser.* 335, 207–216.

Druon, J., Panigada, S., David, L., Gannier, A., Mayol, P., Arcangeli, A., Caadas, A., Laran, S., Mgllo, N.D., Gauffier, P., 2012. Potential feeding habitat of fin whales in the western Mediterranean Sea: an environmental niche model. *Mar. Ecol. Prog. Ser.* 464, 289–306.

Ducet, N., Le Traon, P.Y., Reverdin, G., 2000. Global high-resolution mapping of ocean circulation from TOPEX/Poseidon and ERS-1 and -2. *J. Geophys. Res. Oceans* 105, 19477–19498.

Eckert, S.A., Bagley, D., Kubis, S., Ehrhart, L., Johnson, C., Stewart, K., DeFreese, D., 2006b. Interesting and Postnesting movements and foraging habitats of leatherback Sea turtles (*Dermodochelys coriacea*) nesting in Florida. *Chelonian Conserv. Biol.* 5, 239–248.

Etnoyer, P., Canny, D., Mate, B.R., Morgan, L.E., Ortega-Ortiz, J.G., Nichols, W.J., 2006. Sea-surface temperature gradients across blue whale and sea turtle foraging trajectories off the Baja California Peninsula, Mexico. *Deep Sea Res. Part II Top. Stud. Oceanogr.* 53, 340–358.

Fedak, M.A., Lovell, P., Grant, S.M., 2001. Two approaches to compressing and interpreting time-depth information as collected by time-depth recorders and satellite-linked data recorders. *Mar. Mammal Sci.* 17, 94–110.

Ferraroli, S., Georges, J.-Y., Gaspar, P., Maho, Y.L., 2004. Endangered species: where leatherback turtles meet fisheries. *Nature* 429, 521–522.

Fossette, S., Kelle, L., Girardot, M., Gerverse, E., Hilterman, M.L., Verhage, B., Thoisy, B. de, Georges, J.-Y., 2008. The world's largest leatherback rookeries: a review of conservation-oriented research in French Guiana/Suriname and Gabon. *J. Exp. Mar. Biol. Ecol.* 356, 69–82.

Fossette, S., Hobson, V.J., Girard, C., Calmettes, B., Gaspar, P., Georges, J.-Y., Hays, G.C., 2010b. Spatio-temporal foraging patterns of a giant zooplanktivore, the leatherback turtle. *J. Mar. Syst.* 81, 225–234.

Fossette, S., Girard, C., López-Mendilaharsu, M., Miller, P., Domingo, A., Evans, D., Kelle, L., Plot, V., Prosdocimi, L., Verhage, S., Gaspar, P., Georges, J.-Y., 2010a. Atlantic leatherback migratory paths and temporary residence areas. *PLoS ONE* 5, e13908.

Franeker, J.A., van Brink, N.W., van den Bathmann, U.V., Pollard, R.T., Baar, H.J.W. de, Wolff, W.J., 2002. Responses of seabirds, in particular prions (*Pachyptila* sp.), to small-scale processes in the Antarctic Polar Front. *Deep Sea Res. Part II Top. Stud. Oceanogr.* 49, 3931–3950.

Friedland, K.D., Record, N.R., Asch, R.G., Kristiansen, T., Saba, V.S., Drinkwater, K.F., Henson, S., Leaf, R.T., Morse, R.E., Johns, D.G., Large, S.I., Hjøllø, S.S., Nye, J.A., Alexander, M.A., Ji, R., 2016. Seasonal phytoplankton blooms in the North Atlantic linked to the overwintering strategies of copepods. *Elem. Sci. Anthr.* 4, 99.

Fuglister, F.C., 1963. Gulf stream '60. *Prog. Oceanogr.* 1, 265–373.

Gaspar, P., Georges, J.-Y., Fossette, S., Lenoble, A., Ferraroli, S., Maho, Y.L., 2006. Marine animal behaviour: neglecting ocean currents can lead us up the wrong track. *Proc. R. Soc. B Biol. Sci.* 273, 2697–2702.

Girard, C., Sudre, J., Benhamou, S., Roos, D., Luschi, P., 2006. Homing in green turtles *Chelonia mydas*: oceanic currents act as a constraint rather than as an information source. *Mar. Ecol. Prog. Ser.* 322, 281–289.

Graham, W.M., Pagès, F., Hamner, W.M., 2001. A physical context for gelatinous zooplankton aggregations: a review. *Hydrobiologia* 451, 199–212.

Greer, A.T., Cowen, R.K., Guigand, C.M., McManus, M.A., Sevadjian, J., 2013. Relationships between phytoplankton thin layers and the fine-scale vertical distributions of two trophic levels of zooplankton. *J. Plankton Res.* 35, 939–956.

- Greer, A.T., Cowen, R.K., Guigand, C.M., Hare, J.A., 2015. Fine-scale planktonic habitat partitioning at a shelf-slope front revealed by a high-resolution imaging system. *J. Mar. Syst.* 142, 111–125.
- Hamelin, K.M., Kelley, D.E., Taggart, C.T., James, M.C., 2014. Water mass characteristics and solar illumination influence leatherback turtle dive patterns at high latitudes. *Ecosphere* 5, 1–20.
- Haney, J.C., McGillivray, P.A., 1985. Midshelf fronts in the south atlantic bight and their influence on seabird distribution and seasonal abundance. *Biol. Oceanogr.* 3, 401–430.
- Hays, G.C., Houghton, J.D.R., Myers, A.E., 2004. Endangered species: pan-atlantic leatherback turtle movements. *Nature* 429, (522–522).
- Hays, G.C., Doyle, T.K., Houghton, J.D.R., Lilley, M.K.S., Metcalfe, J.D., Righton, D., 2008. Diving behaviour of jellyfish equipped with electronic tags. *J. Plankton Res.* 30, 325–331.
- Houghton, J.D.R., Doyle, T.K., Wilson, M.W., Davenport, J., Hays, G.C., 2006. Jellyfish aggregations and leatherback turtle foraging patterns in a temperate coastal environment. *Ecology* 87, 1967–1972.
- James, M.C., Mrosovsky, N., 2004. Body temperatures of leatherback turtles (*Dermodochelys coriacea*) in temperate waters off Nova Scotia, Canada. *Can. J. Zool.* 82, 1302–1306.
- James, M.C., Eckert, S.A., Myers, R.A., 2005a. Migratory and reproductive movements of male leatherback turtles (*Dermodochelys coriacea*). *Mar. Biol.* 147, 845–853.
- James, M.C., Myers, R.A., Ottensmeyer, C.A., 2005b. Behaviour of leatherback sea turtles, *Dermodochelys coriacea*, during the migratory cycle. *Proc. R. Soc. Lond. B Biol. Sci.* 272, 1547–1555.
- James, M.C., Davenport, J., Hays, G.C., 2006. Expanded thermal niche for a diving vertebrate: a leatherback turtle diving into near-freezing water. *J. Exp. Mar. Biol. Ecol.* 335, 221–226.
- Kara, A.B., Rochford, P.A., Hurlburt, H.E., 2000a. An optimal definition for ocean mixed layer depth. (July 15) *J. Geophys. Res.* Oceans 105, 16803–16821.
- Kara, A.B., Rochford, P.A., Hurlburt, H.E., 2003. Mixed layer depth variability over the global ocean. *J. Geophys. Res.* Oceans 108, 3079.
- Largier, J.L., 1993. Estuarine fronts: How important are they? *Estuaries* 16, 1–11.
- Lavielle, M., 2005. Using penalized contrasts for the change-point problem. *Signal Process* 85, 1501–1510.
- Le Fèvre, J., 1986. Aspects of the Biology of Frontal Systems, Advances in Marine Biology. Academic Press.
- Lehodey, P., Senina, I., Murtugudde, R., 2008. A spatial ecosystem and populations dynamics model (SEAPODYM) – modeling of tuna and tuna-like populations. *Prog. Oceanogr.* 78, 304–318.
- Lehodey, P., Murtugudde, R., Senina, I., 2010. Bridging the gap from ocean models to population dynamics of large marine predators: a model of mid-trophic functional groups. *Prog. Oceanogr.* 84, 69–84.
- Lentz, S., Shearman, K., Anderson, S., Plueddemann, A., Edson, J., 2003. Evolution of stratification over the New England shelf during the Coastal Mixing and Optics study, August 1996–June 1997. *J. Geophys. Res.* Oceans 108, 3008.
- Longhurst, A., Sathyendranath, S., Platt, T., Caverhill, C., 1995. An estimate of global primary production in the ocean from satellite radiometer data. *J. Plankton Res.* 17, 1245–1271.
- Lopez, R., Malarde, J.-P., Royer, F., Gaspar, P., 2014. Improving argos doppler location using multiple-model kalman filtering. *IEEE Trans. Geosci. Remote Sens.* 52, 4744–4755.
- López-Mendilaharsu, M., Rocha, C.F.D., Miller, P., Domingo, A., Prosdoci, L., 2009. Insights on leatherback turtle movements and high use areas in the Southwest Atlantic Ocean. *J. Exp. Mar. Biol. Ecol.* 378, 31–39.
- Lowther, A.D., Lydersen, C., Biuw, M., Bruyn, P.J.N. de, Hofmeyr, G.J.G., Kovacs, K.M., 2014. Post-breeding at-sea movements of three central-place foragers in relation to submesoscale fronts in the Southern Ocean around Bouvetoya. *Antar. Sci.* 26, 533–544.
- Lozier, M.S., Owens, W.B., Curry, R.G., 1995. The climatology of the North Atlantic. *Prog. Oceanogr.* 36, 1–44.
- Lutcavage, M.E., 1996. Planning your next meal: leatherback travel routes and ocean fronts. NOAA Tech. Memo. NMFS-SEFSC 378, 174–178.
- Marañón, E., Holligan, P.M., Varela, M., Mourão, B., Bale, A.J., 2000. Basin-scale variability of phytoplankton biomass, production and growth in the Atlantic Ocean. *Deep Sea Res. Part Oceanogr. Res. Pap.* 47, 825–857.
- Marshall, J., Plumb, R.A., 2007. Atmosphere Ocean Climate Dynamics: an introduction text, *International Geophysics* 93. AP.
- Martins, A.M., Pelegrí, J.L., 2006. CZCS chlorophyll patterns in the South Atlantic Bight during low vertical stratification conditions. *Cont. Shelf Res.* 26, 429–457.
- McMahon, C.R., Hays, G.C., 2006. Thermal niche, large-scale movements and implications of climate change for a critically endangered marine vertebrate. *Glob. Change Biol.* 12, 1330–1338.
- Molfetti, É., Vilaça, S.T., Georges, J.-Y., Plot, V., Delcroix, E., Scao, R.L., Lavergne, A., Barrioz, S., Santos, F.R. dos, Thoisy, B. de, 2013. Recent demographic history and present fine-scale structure in the Northwest Atlantic leatherback (*Dermodochelys coriacea*) turtle population. *PLOS ONE* 8, e58061.
- Moore, S.E., Watkins, W.A., Daher, M.A., Davies, J.R., Dahlheim, M.E., 2002. Blue whale habitat associations in the Northwest Pacific: analysis of remotely-sensed data using a Geographic Information System. *Oceanography*, 20–25.
- Murase, H., Hakamada, T., Matsuoka, K., Nishiwaki, S., Inagake, D., Okazaki, M., Tojo, N., Kitakado, T., 2014. Distribution of sei whales (*Balaenoptera borealis*) in the subarctic–subtropical transition area of the western North Pacific in relation to oceanic fronts. *Deep Sea Res. Part II Top. Stud. Oceanogr.* 107, 22–28.
- Nordstrom, C.A., Battaile, B.C., Cotté, C., Trites, A.W., 2013. Foraging habitats of lactating northern fur seals are structured by thermocline depths and submesoscale fronts in the eastern Bering Sea. *Deep Sea Res. Part II Top. Stud. Oceanogr.* 88–89, 78–96.
- Olson, D.B., Backus, R.H., 1985. The concentrating of organisms at fronts: a cold-water fish and a warm-core Gulf stream ring. *J. Mar. Res.* 43, 113–137.
- Olson, D.B., Hitchcock, G., Mariano, A., Ashjian, C., Peng, G., Nero, N., Podesta, G., 1994. Life on the edge: marine life and fronts. *Oceanography* 7, 52–60.
- Polovina, J., Uchida, I., Balazs, G., Howell, E.A., Parker, D., Dutton, P., 2006. The Kuroshio extension bifurcation region: a pelagic hotspot for juvenile loggerhead sea turtles. *Deep Sea Res. Part II Top. Stud. Oceanogr.* 53, 326–339.
- Polovina, J.J., Howell, E.A., 2005. Ecosystem indicators derived from satellite remotely sensed oceanographic data for the North Pacific. *ICES J. Mar. Sci. J. Cons.* 62, 319–327.
- Polovina, J.J., Balazs, G.H., Howell, E.A., Parker, D.M., Seki, M.P., Dutton, P.H., 2004. Forage and migration habitat of loggerhead (*Caretta caretta*) and olive ridley (*Lepidochelys olivacea*) sea turtles in the central North Pacific Ocean. *Fish Oceanogr.* 13, 36–51.
- Potter, I.F., Galuardi, B., Howell, W.H., 2011. Horizontal movement of ocean sunfish, *Mola mola*, in the northwest Atlantic. *Mar. Biol.* 158, 531–540.
- Powell, J.R., Ohman, M.D., 2015. Covariability of zooplankton gradients with glider-detected density fronts in the Southern California Current System. *Deep Sea Res. Part II Top. Stud. Oceanogr.* 112, 79–90.
- Reul, N., Chapron, B., Lee, T., Donlon, C., Boutin, J., Alory, G., 2014. Sea surface salinity structure of the meandering Gulf stream revealed by SMOS sensor. *Geophys. Res. Lett.* 41, (2014GL059215).
- Rousseaux, C.S.G., Lowe, R., Feng, M., Waite, A.M., Thompson, P.A., 2012. The role of the Leeuwin Current and mixed layer depth on the autumn phytoplankton bloom off Ningaloo reef, Western Australia. *Cont. Shelf Res.* 32, 22–35.
- Sanchez-Franks, A., Hameed, S., Wilson, R.E., 2015. The Icelandic low as a predictor of the Gulf stream North wall position. *J. Phys. Oceanogr.* 46, 817–826.
- Scales, K.L., Miller, P.I., Hawkes, L.A., Ingram, S.N., Sims, D.W., Votier, S.C., 2014. REVIEW: on the Front Line: frontal zones as priority at-sea conservation areas for mobile marine vertebrates. *J. Appl. Ecol.* 51, 1575–1583.
- Scales, K.L., Miller, P., Varo-Cruz, N., Hodgson, D.J., Hawkes, L.A., Godley, B.J., 2015. Oceanic loggerhead turtles *Caretta caretta* associate with thermal fronts: evidence from the Canary Current large marine ecosystem. *Mar. Ecol. Prog. Ser.* 519, 195–207.
- Scheffer, A., Bost, C., Trathan, P., 2012. Frontal zones, temperature gradient and depth characterize the foraging habitat of king penguins at South Georgia. *Mar. Ecol. Prog. Ser.* 465, 281–297.
- Schmitz, W.J., McCartney, M.S., 1993. On the North Atlantic circulation. *Rev. Geophys.* 31, 29–49.
- Silva, M.A., Jonsen, I., Russel, D.J., Prieto, R., Thompson, D., 2014. Assessing performance of bayesian state-space models fit to argos satellite telemetry locations processed with kalman filtering. *PLoS ONE* 9.
- Sims, D.W., Quayle, V.A., 1998. Selective foraging behaviour of basking sharks on zooplankton in a small-scale front. *Nature* 393, 460–464.
- Skomal, G.B., Zeeman, S.L., Chisholm, J.H., Summers, E.L., Walsh, H.J., McMahon, K.W., Thorrold, S.R., 2009. Transequatorial migrations by basking sharks in the Western Atlantic Ocean. *Curr. Biol.* 19, 1019–1022.
- Strömberg, K.H.P., Smyth, T.J., Allen, J.I., Pitois, S., O'Brien, T.D., 2009. Estimation of global zooplankton biomass from satellite ocean colour. *J. Mar. Syst.* 78, 18–27.
- Sudre, J., Maes, C., Garçon, V., 2013. On the global estimates of geostrophic and Ekman surface currents. *Limnol. Oceanogr. Fluids Environ.* 3, 1–20.
- Thorne, L.H., Read, A.J., 2013. Fine-scale biophysical interactions drive prey availability at a migratory stopover site for *Phalaropus spp.* in the Bay of Fundy, Canada. *Mar. Ecol. Prog. Ser.* 487, 261–273.
- Tomczak, M., Godfrey, J.S., 2013. Regional Oceanography: An Introduction. Elsevier.
- Whitehead, T.O., Kato, A., Ropert-Coudert, Y., Ryan, P.G., 2016. Habitat use and diving behaviour of macaroni *Eudyptes chrysolophus* and eastern rockhopper *E. chrysolophus filholi* penguins during the critical pre-moult period. *Mar. Biol.* 163, 1–20.
- Wilson, S.G., Lutcavage, M.E., Brill, R.W., Genovese, M.P., Cooper, A.B., Everly, A.W., 2004. Movements of bluefin tuna (*Thunnus thynnus*) in the northwestern Atlantic Ocean recorded by pop-up satellite archival tags. *Mar. Biol.* 146, 409–423.
- Witherington, B., 2002. Ecology of neonate loggerhead turtles inhabiting lines of downwelling near a Gulf stream front. *Mar. Biol.* 140, 843–853.
- Witt, M., Broderick, A., Johns, D., Martin, C., Penrose, R., Hoogmoed, M., Godley, B., 2007. Prey landscapes help identify potential foraging habitats for leatherback turtles in the NE Atlantic. *Mar. Ecol. Prog. Ser.* 337, 231–243.